

The PKC family consists of at least 11 isoforms that are classified into three main subfamilies based on their homology and cofactor requirements for activation: the conventional PKC $\alpha$ ,  $\beta$ I,  $\beta$ II and  $\gamma$  subfamily, which is diacylglycerol (DAG)- and calcium-dependent, the novel PKC $\delta$ ,  $\epsilon$ ,  $\theta$  and  $\eta$  subfamily, which is DAG-dependent and calcium-independent, and the atypical PKC $\zeta$ ,  $\lambda$  and  $\iota$  family, which is phospholipid-dependent. There is growing evidence for a fundamental role of the PKC isoforms, PKC $\delta$  (Platten et al., 2003),  $\epsilon$  (Aksoy et al., 2004; Castrillo et al., 2001),  $\eta$  (Chen et al., 1998),  $\iota$  (Mamidipudi et al., 2004), and  $\zeta$  (Hu et al., 2002; Monick et al., 2000), in the regulation of LPS-induced events in macrophages and dendritic cells. However, it is still unknown how PKCs are integrated into the TLR signaling pathway. In this study, we identified PKC $\delta$  as a signaling molecule that binds to TIRAP/Mal. Functional analysis suggests that PKC $\delta$  participates in the activation of both NF- $\kappa$ B and MAPK cascades induced by TLR signaling.

## 2. Materials and methods

### 2.1. Materials

LPS (*E. coli*, serotype 0111: B4), bovine serum albumin (fatty acid free), GF109203X, staurosporine, histone III-S, poly I:C, and ATP were purchased from Sigma (St. Louis, MO). Phosphatidylserine and phosphatidylinositol were bought from Matreya (Pleasant Gap, PA), raytide, a peptide substrate of tyrosine kinases, was purchased from Oncogene Science (Uniondale, NY), rGM-CSF came from PeproTech EC (London, UK); glutathione–sepharose CL-4B and pGEX-4T-2 were bought from Amersham Biosciences (UK), antibodies raised against PKCs were bought from Transduction Laboratories (Lexington, KY), anti-phospho-p38 MAPK, anti-phospho-SAPK/JNK, and anti-phospho-IKK were bought from cell signaling (Beverly, MA), and anti-phospho-I $\kappa$ B came from Santa Cruz (Santa Cruz, CA). Anti-TIRAP/Mal and anti-IRAK polyclonal antibodies were prepared by immunizing rabbits with full-length rTIRAP/Mal or recombinant C-terminal IRAK-1 peptide (636-end), respectively. [ $\gamma$ - $^{32}$ P]ATP was purchased from New England Nuclear, and Phos-tag (1,3-bis[bis(pyridine-2-ylmethyl)amino]propan-2-olato dizinc(II) complex (Kinoshita et al., 2006) was kindly donated by Dr. T. Koike (Hiroshima University).

### 2.2. Plasmids

Total RNA was extracted from human monocytes that had been cultured for 10 days with 10 ng/ml GM-CSF using an RNeasy Mini Kit (Qiagen) according to the manufacturer's protocol. Complementary DNA from TIRAP/Mal, IRAK-1, and MyD88 were amplified by RT-PCR using primers based on the sequences of the GenBank accession numbers AF406652, L76191 and U70451, respectively. The coding sequences for TIRAP/Mal and MyD88 were subcloned into pGEX-4T-2 in-frame with the GST coding sequence. TIRAP/Mal was also cloned into pcDNA3.1 with an N-terminal HA-tag. pcDNA3-FLAG-PKC $\delta$  (GenBank accession number M18330) was kindly

donated by Dr. Yoshitaka Ono (Biomedical Research Center, Kobe). Truncation mutants of HA-Mal were made by PCR.

### 2.3. Cells

HEK293T cells were maintained in Dulbecco's modified Eagle's medium (DMEM; Nissui, Japan) supplemented with 10% FCS in humidified 5% CO $_2$  at 37 °C. A mouse macrophage-like cell line, RAW264.7, was maintained in RPMI1640 medium fortified with 2.5 g/L glucose and 10% FCS in humidified 5% CO $_2$  at 37 °C. Peritoneal macrophages were harvested from female Donryu rats. Briefly, animals were injected intraperitoneally with 20 ml of a 3% thioglycollate broth. After 4 days, peritoneal exudate cells were harvested by washing the peritoneal cavity with ice-cold PBS. The cells were resuspended in RPMI1640 medium supplemented with 10% FCS and seeded at approximately,  $1.5 \times 10^7$  cells/10-cm dish for the pull-down assay, or  $3 \times 10^6$  cells/well of a 6-well plate for immunoprecipitation, and incubated in humidified 5% CO $_2$  at 37 °C for 1–2 h. Non-adherent cells were removed by washing vigorously with PBS and the attached cells were used as macrophages. Macrophages were incubated in humidified 5% CO $_2$  at 37 °C in the presence or absence of LPS.

### 2.4. Transfection

293T cells were cultured in 6-well plates prior to the protein-protein interaction assay. The cells were seeded at  $5 \times 10^5$  cells/well for 24 h before transfection using FuGENE 6 (Roche) according to the manufacturer's protocol. After 24 h, cells were lysed for immunoprecipitation. To detect expression of IRAKs and PKCs, 293T cells were plated at  $5 \times 10^5$  cells/10-cm dish for 24 h before calcium phosphate transfection. The media was changed 20–24 h after transfection, and 48 h later the cells were lysed for immunoprecipitation.

### 2.5. GST-fusion proteins

BL21 (DE3) cells were transformed with the GST-TIRAP/Mal or GST-MyD88 plasmid, and grown to mid-log phase. Protein production was induced with 1 mM isopropyl-1-thio- $\beta$ -D-galactopyranoside for 4 h at 30 °C. The cells were harvested by centrifugation, lysed with lysis buffer (TBS containing 0.5% Triton X-100 and 1 mM PMSF), and sonicated 3  $\times$  for 30 s with a needle sonicator at 40–50% power. The clarified supernatants were incubated with glutathione–sepharose at 4 °C for 60 min. The beads containing the recombinant proteins were washed six times with lysis buffer.

### 2.6. Pull-down with GST-proteins

After removal of cell culture supernatants, the cells were washed once with ice-cold PBS containing 1 mM EDTA, 10 mM NaF and 1 mM Na $_3$ VO $_4$ , and immediately incubated in 1 ml of lysis buffer (1 mM EDTA, 25 mM Tris-HCl (pH 7.4), 100 mM NaCl, 30 mM NaF, 1% Nonidet P-40, 1 mM Na $_3$ VO $_4$ , 1 mM PMSF, 2  $\mu$ M leupeptin, and 20  $\mu$ M PA-PMSF)

for 10 min on ice. The cell lysates were centrifuged at 15,000 rpm for 10 min. The resultant supernatants were precleared with glutathione–sepharose at 4 °C for 60 min and incubated with the GST-fusion proteins immobilized on glutathione–sepharose at 4 °C for 120 min. The sepharose beads with the fusion proteins were spun briefly in a microfuge and washed four times with ice-cold lysis buffer. For the *in vitro* kinase assay, the beads were further washed with kinase assay buffer (25 mM Tris–HCl, pH 7.5, 0.1 mM EDTA, and 0.1 mg/ml BSA).

### 2.7. Immunoprecipitation

Cell lysates were prepared as above, and incubated with the appropriate antiserum for at least 60 min on ice. A slurry of pre-washed protein A–Sepharose CL-4B (30% slurry, 50  $\mu$ l) was added to each sample and incubated on a rotator at 4 °C for an additional 2 h. The samples were spun briefly in a microfuge and washed four times with ice-cold lysis buffer. For the *in vitro* kinase assay, the beads were further washed with kinase assay buffer as described above.

### 2.8. *In vitro* kinase assay

The kinase activities of the GST-TIRAP/Mal and GST-MyD88 fusion proteins were determined by incubating the glutathione-beads with [ $\gamma$ -<sup>32</sup>P]ATP and protein substrates. The glutathione-beads were suspended in 20  $\mu$ l kinase assay buffer containing the appropriate substrates and protein kinase inhibitors. Unless otherwise specified, phospholipids were added to the reaction mixture as lipid vehicles made by sonication. The reaction was initiated by adding 10  $\mu$ l of the reaction mixture fortified with 0.3 mM [ $\gamma$ -<sup>32</sup>P]ATP (1  $\mu$ Ci), 5  $\mu$ g histone III-S and 30 mM MgCl<sub>2</sub>, continued at 30 °C for 60 min, and terminated by addition of SDS sample buffer. After separation of the proteins on SDS-PAGE, the gels were stained with coomassie brilliant blue (CBB) and the protein bands were analyzed with an imaging analyzer to estimate the degree of substrate phosphorylation. Anti-IRAK and anti-flag-PKC immunoprecipitates were also assessed using the methodology described above.

### 2.9. Western blotting

GST-fusion proteins immobilized on glutathione–sepharose beads, anti-TIRAP/Mal immunoprecipitates, anti-flag immunoprecipitates of PKC $\delta$ , or total cell lysates were heated at 100 °C for 3 min in 30  $\mu$ l of the sample buffer containing 62.5 mM Tris (pH 6.8), 1% SDS, 10% glycerol, 5% 2-mercaptoethanol, and 0.02% bromophenol blue. The proteins were separated by SDS-PAGE on a 10% slab gel and transferred electrophoretically to a polyvinylidene difluoride (PVDF) membrane (Millipore). The membranes were blocked, incubated with the appropriate antibodies, and visualized by enhanced chemiluminescence.

### 2.10. RNA interference

Two sets of oligonucleotides were cloned into the pH1 vector to express PKC $\delta$  siRNA hairpins downstream of the human

H1 RNA promoter, as described previously (Sasai et al., 2005). The following sequences were used: 5'-GAACGCTTCAAC-ATCGACA-3 and 5'-GGCCGTGTTATCCAGATTG-3. HEK-293T cells were transfected with 100 ng of pH1-empty or 50 ng of each pH1-siPKC $\delta$  vector using FuGENE6 transfection reagent. About 5–10  $\times$  10<sup>6</sup> RAW264.7 cells were transfected by electroporation in a 300  $\mu$ l final volume at 250 V/950  $\mu$ F (Gene Pulser II, Bio-Rad). Puromycin (2  $\mu$ g/ml for 293T cells and 5  $\mu$ g/ml for RAW264.7 cells) was added to the cells 24 h after transfection and incubation was continued for several days. Puromycin-resistant colonies were replated. To determine the efficiency of gene silencing, total RNA was isolated with RNeasy (Qiagen, Hilden, Germany) and mRNA was assessed by RT-PCR.

## 3. Results

### 3.1. GST-TIRAP/Mal fusion protein associates with protein kinases

We first determined whether TIRAP/Mal interacts with protein kinases. Recombinant GST-TIRAP/Mal was incubated with rat peritoneal macrophage lysates. Proteins associating with the fusion protein were analyzed in the *in vitro* kinase assay using histone III-S as a substrate. Phosphorylation of histone III-S was prominent when phospholipids were included in the assay mixture (Fig. 1, upper panel). TIRAP/Mal and histone III-S levels remained unchanged during the kinase assay (Fig. 1, lower panel), and GST alone was not associated with protein kinases activity (Fig. 1B). A tyrosine kinase substrate, raytide, was not phosphorylated by TIRAP/Mal-associated kinase (data not shown). Since PKC family members are phospholipid-dependent, we tested the effect of PKC inhibitors on the protein kinase activities. A PKC inhibitor with a broad spectrum, GF109203X, inhibited histone III-S phosphorylation by TIRAP/Mal-associated kinases, while Gö6976, a specific inhibitor of conventional PKCs, did not (Fig. 2A, upper panels). MyD88 also associated with some protein kinases, as shown by histone III-S phosphorylation (Fig. 2B). MyD88-associated activity was susceptible to both GF109203X and Gö6976 (Fig. 2B, upper panels) indicating that the bound kinases are different from those associated with TIRAP/Mal. Another PKC inhibitor, staurosporine, strongly inhibited both MyD88-associated and TIRAP/Mal-associated kinases (data not shown). Since MyD88 is known to bind IRAK family members, we analyzed these as potential TIRAP/Mal-associated protein kinases. However, GF109203X, which inhibited protein kinase activity associated with TIRAP/Mal (Fig. 2A, left upper panel), failed to inhibit kinase activity in lysates from IRAK-1 and IRAK-4 transfected 293T cells (data not shown).

### 3.2. Identification of PKC $\delta$ and $\eta$ as TIRAP/Mal-associated kinases

Whole cell lysates of rat macrophages were western blotted with a series of specific antibodies against the PKC isoforms. As shown in Fig. 3A, PKC $\delta$ ,  $\iota$ , and  $\lambda$  were the dominant PKC

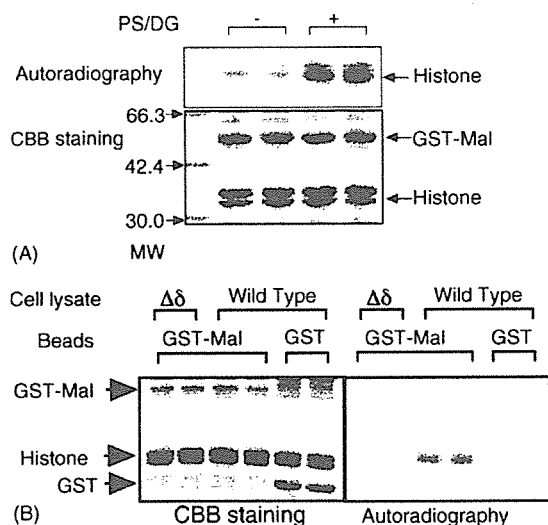


Fig. 1. Association of protein kinase activity with GST-TIRAP/Mal. (A) GST-TIRAP/Mal immobilized on glutathione–Sepharose beads were incubated with rat macrophage lysates. The beads were washed four times and assayed for protein kinase activity using  $[\gamma\text{-}^{32}\text{P}]\text{ATP}$  and histone III-S as substrates in the presence (+) or absence (–) of phosphatidylserine and diacylglycerol (PS/DG). The reaction was terminated by the addition of SDS sample buffer. (B) GST-TIRAP/Mal or control GST immobilized on glutathione–sepharose were incubated with lysates from wild type RAW264.7 cells or PKC $\delta$  deficient cells ( $\Delta\delta$ ). Protein kinase activity associated with the beads was determined in the presence of the phospholipids. (A and B) The phosphorylated proteins were visualized using an imaging analyzer (Autoradiography). Histone III-S and the fusion proteins were stained with CBB on the same gels. Positions of molecular mass markers (kDa) are indicated on the left of the panel, while the positions of the proteins are indicated on the right in (A). The position of the proteins are indicated on the left of the panel in (B).

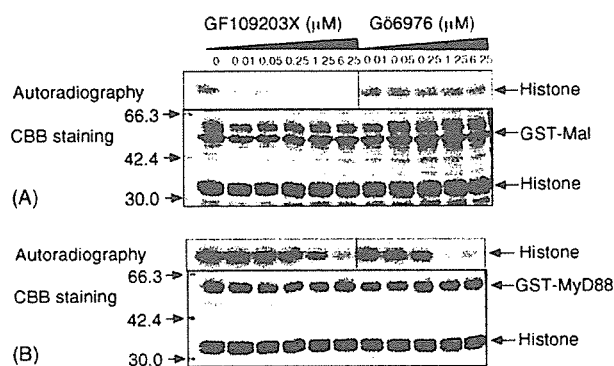


Fig. 2. Effects of PKC inhibitors on the protein kinase activity bound to GST-TIRAP/Mal and GST-MyD88. GST-TIRAP/Mal (A) or GST-MyD88 (B) immobilized on glutathione–sepharose was incubated with rat macrophage lysates. The beads were washed and assayed for protein kinase activity using  $[\gamma\text{-}^{32}\text{P}]\text{ATP}$  and histone III-S. Increasing concentrations of GF109203X or G66976 were added to the assay mixture. Protein phosphorylation was visualized with an imaging analyzer (upper panels). The amounts of histone III-S and fusion proteins on the same gels were detected by CBB staining (lower panels). Positions of the molecular mass markers (kDa) are indicated on the left of the panels, while the positions of the proteins are indicated on the right.

subtypes observed by the employed antibodies, though PKC $\alpha$  and  $\beta$  were also observed. The lysates were mixed with GST-TIRAP/Mal immobilized on glutathione–sepharose beads, and protein associated with the beads was western blotted with specific antibodies. PKC $\delta$  and  $\eta$  bound GST-TIRAP/Mal (Fig. 3A), while GST alone did not bind any PKCs (data not shown). A point mutation of TIRAP/Mal (P125H) known to impair the ability of this adaptor to bind TLR4 and MyD88 (Hornig et al., 2001; Fitzgerald et al., 2001; Xu et al., 2000), did not alter the ability of TIRAP/Mal to bind PKC $\delta$  and  $\eta$  (Fig. 3A). PKC $\delta$  and  $\eta$  binding to TIRAP/Mal was also observed in the lysates of monocytic THP-1 cells (data not shown).

To confirm the binding of TIRAP/Mal to PKC $\delta$ , RAW264.7 cells were transfected with shRNA probes that targeted PKC $\delta$ . The probes prevented PKC $\delta$  expression without affecting expression of a control protein, p67<sup>phox</sup> (Fig. 5). Lysates of PKC $\delta$ -depleted cells were incubated with recombinant GST-TIRAP/Mal and protein associated with this fusion protein was assessed using the *in vitro* kinase assay. Depletion of PKC $\delta$  markedly decreased the protein kinase activity associated with GST-TIRAP/Mal (Fig. 1B). As shown in Fig. 3B, a polyclonal antibody against TIRAP/Mal was used to analyze its interaction with PKC $\delta$ . This antibody was incubated with rat peritoneal macrophage lysates, and the immune complex was analyzed using a monoclonal antibody against PKC $\delta$ . The results confirmed that TIRAP/Mal associates with PKC $\delta$  and showed that this association is constitutive, remaining unchanged after treatment with LPS. The anti-TIRAP/Mal antibody precipitated the histone III-S kinase activity from wild type RAW264.7 cell lysates (Fig. 3C), and kinase activity also remained unchanged by LPS treatment. When a similar experiment was performed using the lysate from PKC $\delta$ -deficient cells, kinase activity was barely detected in the immune complex (Fig. 3C). As shown in Fig. 3D, RAW264.7 cell lysates were mixed with anti-PKC $\delta$ , and the immune complex was analyzed by Phos-tag, a probe used to detect phosphorylated proteins (Kinoshita et al., 2006). The proteins in the immune complex of anti-PKC $\delta$  were separated by SDS-PAGE, transferred to PVDF membrane, and analyzed by Phos-tag. Interestingly, LPS increased the phosphorylation of several proteins in the immune complex. PKC $\delta$  was constitutively phosphorylated, however, the level of phosphorylation was unaffected by LPS treatment.

293T cells were then transfected with flag-PKC $\delta$  along with HA-TIRAP/Mal (Fig. 4). The cell lysate was mixed with an anti-flag antibody, and immune complexes were analyzed using an anti-HA antibody. The results confirmed that PKC $\delta$  binds to the full length TIRAP/Mal (WT). The TIR domain of TIRAP/Mal (86 to end) bound flag-PKC $\delta$ , while HA-TIRAP/Mal lacking the TIR domain ( $\Delta\text{TIR}$ ) did not complex with flag-PKC $\delta$ .

### 3.3. Possible involvement of PKC $\delta$ in LPS-induced activation of MAPKs and IKK

TLR ligation is known to activate MAPKs and IKK. As shown in Fig. 5A, stimulation of RAW264.7 cells with LPS, a TLR4 ligand, induced the phosphorylation of IKK, p38 MAPK,

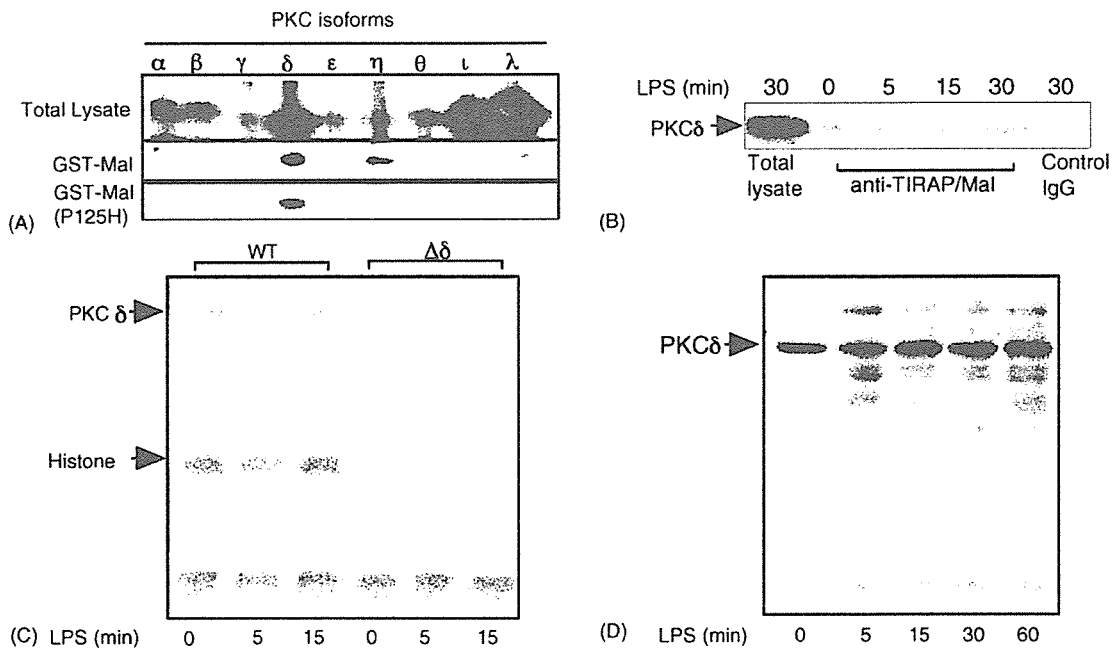


Fig. 3. PKC $\delta$  binds GST-TIRAP/Mal. (A) GST-TIRAP/Mal or its mutant (P125H) immobilized on glutathione-sepharose were incubated with rat macrophage lysates. The bound proteins were analyzed by immunoblotting with a series of anti-PKC antibodies as indicated at the top of the panel. Total macrophage lysate was also immunoblotted (top panel). (B) Rat macrophages were stimulated with 100 ng/ml LPS for the times indicated at the top of the panel. The cell lysates were immunoprecipitated with anti-TIRAP/Mal antibody or control IgG and the proteins in the immune complex were analyzed by immunoblotting with anti-PKC $\delta$ . Total cell lysates were also analyzed as a positive control. The positions of PKC $\delta$  and TIRAP/Mal are indicated on the left of the panel. (C) Wild type RAW264.7 cells or PKC $\delta$ -deficient cells ( $\Delta\delta$ ) were stimulated with LPS. The lysates were immunoprecipitated with anti-Mal antibody and the immunoprecipitates were analyzed by *in vitro* kinase assay. (D) Wild type RAW264.7 cells were stimulated with 100 ng/ml LPS. The cell lysates were immunoprecipitated with anti-PKC $\delta$  antibody and phosphorylated proteins were detected using Phos-tag.

and I $\kappa$ B. The LPS-induced events were completely abolished in PKC $\delta$ -deleted cells (Fig. 5A). Similar results were obtained in cells treated with Malp2, a TLR2/TLR6 ligand (Fig. 5B). These results indicate that PKC $\delta$  plays a critical role in TIRAP/Mal-dependent signaling pathways. Poly I:C is a TLR3 ligand that

binds TICAM-1 but not TIRAP/Mal. Poly I:C, like LPS and Malp2, induced the phosphorylation of IKK, p38 MAPK, and I $\kappa$ B (Fig. 5C). In PKC $\delta$ -deficient cells, IKK and I $\kappa$ B phosphorylation were severely impaired but still observable (Fig. 5C). Interestingly, the phosphorylation of p38 MAPK was not altered by the 60–90 min treatment (Fig. 5C). Phosphorylation induced by calyculin A, a pan-inhibitor of Ser/Thr phosphatases, was not affected by PKC $\delta$ -depletion (Fig. 5D).

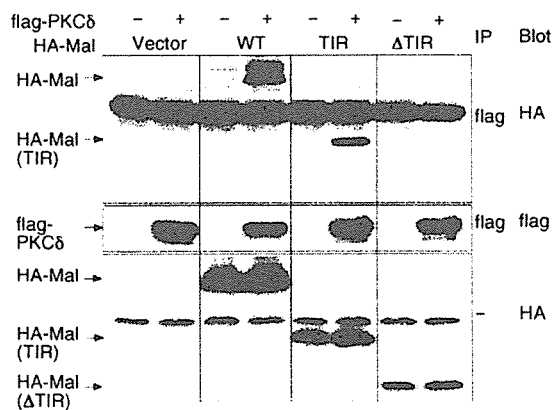


Fig. 4. The TIR domain of TIRAP/Mal associates with PKC $\delta$ . 293T cells were transfected with 0.5  $\mu$ g of flag-PKC $\delta$  with HA-TIRAP/Mal (WT), HA-TIRAP/Mal-TIR (TIR, 86-end), or HA-TIRAP/Mal- $\Delta$ TIR ( $\Delta$ TIR, 1–85) as indicated. PKC $\delta$  was immunoprecipitated from the cell lysates with an anti-flag antibody. The proteins in the immune complex were separated by SDS-PAGE and blotted with an anti-HA antibody (top panel) or anti-flag antibody (middle panel). The amount of HA-TIRAP/Mal in the total cell lysate was determined by blotting with an anti-HA antibody (lower panel). The positions of the proteins are indicated on the left of the panel.

#### 4. Discussion

Numerous studies have reported that LPS induces PKC activation (Aksoy et al., 2004; Shinji et al., 1994). A deficiency in LPS-induced translocation of novel and conventional PKC is observed in macrophages from C3H/HeJ mice, which harbor a TLR4 point mutation (Shinji et al., 1994). PKC $\zeta$ , an atypical PKC subfamily member, is proposed to function in LPS-induced IRAK activation (Hu et al., 2002), and PKC $\epsilon$ , a novel PKC, is indispensable for LPS-induced IL-12 production by dendritic cells (Aksoy et al., 2002). PKC $\epsilon$ -deficient murine macrophages display a major defect in their capacity to clear bacterial infection (Castrillo et al., 2001).

It is reported that LPS-induced activation of NF- $\kappa$ B is inhibited by rottlerin (Kontny et al., 2000). Although rottlerin is often utilized as an inhibitor of PKC $\delta$ , a recent study indicated that the compound do not inhibit PKC $\delta$  (Davies et al., 2000). We confirmed the inability of rottlerin to inhibit PKC $\delta$  using a

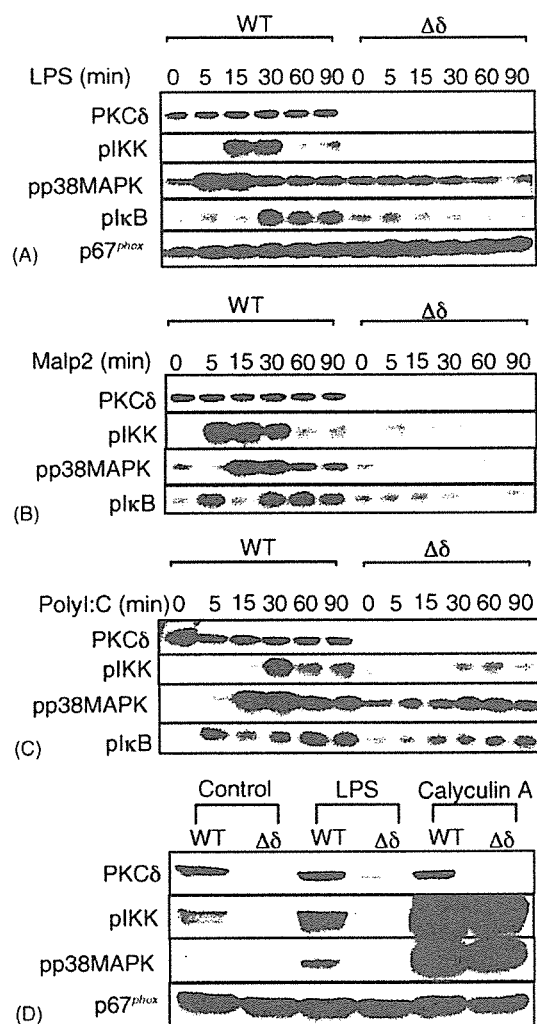


Fig. 5. Possible involvement of PKC $\delta$  in TLR-mediated activation of p38MAPK and NF- $\kappa$ B. RAW264.7 cells were transfected with two PKC $\delta$ -shRNAs (10  $\mu$ g each) or empty vector (20  $\mu$ g) by electroporation. After 24 h, 7  $\mu$ g/mL of puromycin was added and the cells were cultured for 4 weeks, changing the medium every 5 days. The resistant colonies were plated in fresh medium without puromycin and cultured for an additional 24 h. The cells were stimulated with 10 ng/ml of LPS (A), 0.1  $\mu$ M of Malp2 (B), or 25  $\mu$ g/mL of Poly I:C (C) for the times indicated at the top of the panels. (D) Cells were treated with 0.1  $\mu$ M calyculin A for 15 min. The cell lysates were western blotted with the antibodies indicated at the left of the panels.

recombinant enzyme (data not shown). Thus, the present study was performed to provide a new line of evidence suggesting that PKC $\delta$  is involved in TLR signaling. We observed that the adaptor protein, TIRAP/Mal, is associated with protein kinase activity (Fig. 2) that is unaffected by rottlerin (data not shown). The effects of phospholipid and pharmacological inhibitors suggested involvement of PKC family members. Immunological analysis indicated that PKC $\delta$  and  $\eta$ , members of the novel PKC subfamily, were associating with TIRAP/Mal (Fig. 3A). Indeed, truncated mutants of TIRAP/Mal showed that the TIR domain is required for binding to PKC $\delta$  (Fig. 4). PKC $\epsilon$ , another novel isoform, is recently shown to be a critical component of the TLR4 signaling pathway (Aksoy et al., 2002). It appears that some

structures that are common in novel PKC family members may associate favorably with TIRAP/Mal.

Constitutively active PKC $\theta$ , another novel PKC isoform, is a potent activator of NF- $\kappa$ B and AP-1 in Jurkat T cells (Lin et al., 2000; Baier-Bitterlich et al., 1996). Activation of IKK and NF- $\kappa$ B by TCR signaling depends on PKC $\beta$  or novel PKCs (Shinohara et al., 2005; Sommer et al., 2005; Krappmann et al., 2001). Although this finding suggests that novel PKCs are involved in the signaling pathway leading to NF- $\kappa$ B activation, it is not clear whether each PKC isozyme has a specialized function. The substrate specificity of PKC isoforms is redundant, so their physiological roles in certain cell types may depend on their relative abundance, localization, and cellular environment. In this study, we observed that TLR2- and TLR4-mediated activation of IKK was completely abolished in PKC $\delta$ -deficient RAW264.7 cells (Fig. 5). Considering that PKC $\delta$  is the most abundant novel PKC in macrophages, it is not surprising that this subtype plays a dominant role in these cells. In fact, activation of NF- $\kappa$ B by TLR2, TLR4, TLR3, and TLR9 was also attenuated in PKC $\delta$ -deficient cells (data not shown). TLR3-mediated responses were attenuated but still observed in these cells, while the TLR2/4 responses were completely abolished (Fig. 5). Therefore, we have to consider two independent roles of PKC $\delta$  in TLR signaling. One is specific for TLR2/4, and another is common to all TLRs.

TICAM-1/TRIF did not bind to PKC $\delta$  (data not shown). In addition, ligation of TLR3 with polyI:C did not increase the phosphorylation of PKC $\delta$ -associated proteins (data not shown) where TLR4 ligation considerably increase the phosphorylation (Fig. 3D). It is very likely that PKC $\delta$  interacts specifically with TIRAP/Mal. There may be another mechanism by which PKC $\delta$  regulates TLR-mediated signals. We have recently observed that phosphatidylinositol 3-kinase (PI3K) and Akt activity is greatly increased in the PKC $\delta$  deficient cells (to be published elsewhere). As reported by numerous studies and also by us, activation of PI3K/Akt resulted in a suppression of TLR-mediated NF- $\kappa$ B activation. The negative regulation by PI3K of TLR is commonly observed with all TLR signals (Hazeki et al., 2006). Based on this, the augmentation of PI3K activity in PKC $\delta$  deficient cells may be responsible for the general impairment of TLR signals.

TIRAP/Mal is only shared by TLR2 and TLR4, while MyD88 is shared by all the TLRs (Yamamoto et al., 2003). Thus, TIRAP/Mal-binding proteins are good candidates for a signaling molecule that induces specific responses to TLR2 and TLR4. Although the signaling pathway downstream of MyD88 is well characterized, little is known about TIRAP/Mal signaling except that it specifically associates with PKR (Hornig et al., 2001) and IRAK-2 (Fitzgerald et al., 2001). This study suggests that PKC $\delta$  also interacts specifically with TIRAP/Mal. Interactions between TIRAP/Mal and Btk, a Tec family tyrosine kinase, are also reported. TIRAP/Mal is phosphorylated by Btk and subject to proteosomal degradation, which results in negative feedback termination of the innate immune response (Mansell et al., 2006). Interestingly, PKC $\delta$  inhibits the function of Tec family tyrosine kinases (Saharinen et al., 1997). It is intriguing to consider that the inhibition of Btk is one of the

specialized functions of PKC $\delta$ . Another recent study revealed that TIRAP/Mal associates with TRAF6 (Mansell et al., 2004), which binds to numerous functional proteins including MyD88 (Kawai et al., 2004), IRAK-1 (Jiang et al., 2002), TRIF (TICAM-1; Sato et al., 2003), TBK-1 (Sato et al., 2003), TAB1/2 (Qian et al., 2001), TAK-1 (Qian et al., 2001), IRF-7 (Kawai et al., 2004), ECSIT (Kopp et al., 1999),  $\beta$ -arrestin (Wang et al., 2006), Src family tyrosine kinase (Wong et al., 1999), Ras (McDermott and O'Neill, 2002), and aPKC-interacting p62 (Sanz et al., 2000). These proteins are candidates for regulation by PKC $\delta$ , as described below.

We showed that LPS increases the association between phosphorylated proteins and PKC $\delta$  (Fig. 3D). PKC $\delta$  is activated when tyrosine residues on this protein become phosphorylated (Konishi et al., 2001). Since ligation of TLR4 increases tyrosine kinase activity in cells (Hazeki et al., 2003), it is possible that tyrosine-phosphorylated PKC $\delta$  phosphorylates other proteins. We did not observe any effect of LPS on the tyrosine-phosphorylation of PKC $\delta$ , however (data not shown), and the PKC $\delta$  activity associated with TIRAP/Mal was also unaffected by LPS (Fig. 3C). Another possibility is that PKC $\delta$  is recruited to the TLR signaling complex, since PKC translocation is often observed in intact cells. We have observed that the association between PKC $\delta$  and TIRAP/Mal is not dependent on receptor ligation (Fig. 3B). Thus, LPS-induced recruitment of TIRAP/Mal to the TLR or TRAF6 may be the event that results in increased phosphorylation of proteins in the immune complex formed by anti-PKC $\delta$ . LPS induces the association between TIRAP/Mal and TRAF6, which binds to PKC $\delta$  and its substrates, respectively. Further study is necessary to define the detailed signaling mechanism.

#### Acknowledgments

We thank Dr. Yoshitaka Ono (Biosignal Research Center, Kobe) and Dr. T. Koike (Hiroshima University) for the generous gift of PKC $\delta$  plasmid and Phos-tag, respectively. This work was carried out with kind cooperation from the Research Center for Molecular Medicine, Faculty of Medicine, Hiroshima University.

#### Appendix A. Supplementary data

Supplementary data associated with this article can be found, in the online version, at doi:10.1016/j.molimm.2006.11.005.

#### References

- Akira, S., 2003. Toll-like receptor signaling. *J. Biol. Chem.* 278, 38105–38108.
- Aksoy, E., Amraoui, Z., Goriely, S., Goldman, M., Willems, F., 2002. Critical role of protein kinase C epsilon for lipopolysaccharide-induced IL-12 synthesis in monocyte-derived dendritic cells. *Eur. J. Immunol.* 32, 3040–3049.
- Aksoy, E., Goldman, M., Willems, F., 2004. Protein kinase C epsilon: a new target to control inflammation and immune-mediated disorders. *Int. J. Biochem. Cell Biol.* 36, 183–188.
- Baier-Bitterlich, G., Uberall, F., Bauer, B., Fresser, F., Wachter, H., Grunick, H., Utermann, G., Altman, A., Baier, G., 1996. Protein kinase C-theta isoenzyme selective stimulation of the transcription factor complex AP-1 in T lymphocytes. *Mol. Cell Biol.* 16, 1842–1850.
- Castrillo, A., Pennington, D.J., Otto, F., Parker, P.J., Owen, M.J., Bosca, L., 2001. Protein kinase Cepsilon is required for macrophage activation and defense against bacterial infection. *J. Exp. Med.* 194, 1231–1242.
- Chen, C.C., Wang, J.K., Chen, W.C., Lin, S.B., 1998. Protein kinase C eta mediates lipopolysaccharide-induced nitric-oxide synthase expression in primary astrocytes. *J. Biol. Chem.* 273, 19424–19430.
- Davies, S.P., Reddy, H., Caivano, M., Cohen, P., 2000. Specificity and mechanism of action of some commonly used protein kinase inhibitors. *Biochem. J.* 351, 95–105.
- Fitzgerald, K.A., Palsson-McDermott, E.M., Bowie, A.G., Jefferies, C.A., Mansell, A.S., Brady, G., Brint, E., Dunne, A., Gray, P., Harte, M.T., McMurray, D., Smith, D.E., Sims, J.E., Bird, T.A., O'Neill, L.A., 2001. Mal (MyD88-adaptor-like) is required for toll-like receptor-4 signal transduction. *Nature* 413, 78–83.
- Hazeki, K., Masuda, N., Funami, K., Sukenobu, N., Matsumoto, M., Akira, S., Takeda, K., Seya, T., Hazeki, O., 2003. Toll-like receptor-mediated tyrosine phosphorylation of paxillin via MyD88-dependent and -independent pathways. *Eur. J. Immunol.* 33, 740–747.
- Hazeki, K., Kinoshita, S., Matsumura, T., Nigorikawa, K., Kubo, H., Hazeki, O., 2006. Opposite effects of wortmannin and 2-(4-morpholinyl)-8-phenyl-1(4H)-benzopyran-4-one hydrochloride on toll-like receptor-mediated nitric oxide production: negative regulation of nuclear factor- $\kappa$ B by phosphoinositide 3-kinase. *Mol. Pharmacol.* 69, 1717–1724.
- Hornig, T., Barton, G.M., Medzhitov, R., 2001. TIRAP: an adapter molecule in the toll signaling pathway. *Nat. Immunol.* 2, 835–841.
- Hu, J., Jacinto, R., McCall, C., Li, L., 2002. Regulation of IL-1 receptor-associated kinases by lipopolysaccharide. *J. Immunol.* 168, 3910–3914.
- Jiang, Z., Ninomiya-Tsuji, J., Qian, Y., Matsumoto, K., Li, X., 2002. Interleukin-1 (IL-1) receptor-associated kinase-dependent IL-1-induced signaling complexes phosphorylate TAK1 and TAB2 at the plasma membrane and activate TAK1 in the cytosol. *Mol. Cell Biol.* 22, 7158–7167.
- Kaisho, T., Akira, S., 2001. Dendritic-cell function in toll-like receptor- and MyD88-knockout mice. *Trends Immunol.* 22, 78–83.
- Kawai, T., Sato, S., Ishii, K.J., Coban, C., Hemmi, H., Yamamoto, M., Terai, K., Matsuda, M., Inoue, J., Uematsu, S., Takeuchi, O., Akira, S., 2004. Interferon-alpha induction through Toll-like receptors involves a direct interaction of IRF7 with MyD88 and TRAF6. *Nat. Immunol.* 5, 1061–1068.
- Kinoshita, E., Kinoshita-Kikuta, E., Takiyama, K., Koike, T., 2006. Phosphate-binding tag, a new tool to visualize phosphorylated proteins. *Mol. Cell Proteom.* 5, 749–757.
- Konishi, H., Yamauchi, E., Taniguchi, H., Yamamoto, T., Matsuzaki, H., Take-mura, Y., Ohmae, K., Kikkawa, U., Nishizuka, Y., 2001. Phosphorylation sites of protein kinase C delta in H<sub>2</sub>O<sub>2</sub>-treated cells and its activation by tyrosine kinase in vitro. *Proc. Natl. Acad. Sci. USA* 98, 6587–6592.
- Kontny, E., Kurowska, M., Szczepanska, K., Maslinski, W., 2000. Rottlerin, a PKC isozyme-selective inhibitor, affects signaling events and cytokine production in human monocytes. *J. Leukoc. Biol.* 67, 249–258.
- Kopp, E., Medzhitov, R., Carothers, J., Xiao, C., Douglas, I., Janeway, C.A., Ghosh, S., 1999. ECSIT is an evolutionarily conserved intermediate in the Toll/IL-1 signal transduction pathway. *Genes Dev.* 13, 2059–2071.
- Krappmann, D., Patke, A., Heissmeyer, V., Scheidereit, C., 2001. B-cell receptor- and phorbol ester-induced NF-kappaB and c-Jun N-terminal kinase activation in B cells requires novel protein kinase C's. *Mol. Cell Biol.* 21, 6640–6650.
- Lin, X., O'Mahony, A., Mu, Y., Gelezianus, R., Greene, W.C., 2000. Protein kinase C-theta participates in NF-kappaB activation induced by CD3-CD28 costimulation through selective activation of IkappaB kinase beta. *Mol. Cell Biol.* 20, 2933–2940.
- Mamidiipudi, V., Lin, C., Seibenhener, M.L., Wooten, M.W., 2004. Regulation of interleukin receptor-associated kinase (IRAK) phosphorylation and signaling by iota protein kinase C. *J. Biol. Chem.* 279, 4161–4165.
- Mansell, A., Brint, E., Gould, J.A., O'Neill, L.A., Hertzog, P.J., 2004. Mal interacts with tumor necrosis factor receptor-associated factor (TRAF)-6 to mediate NF-kappaB activation by toll-like receptor (TLR)-2 and TLR4. *J. Biol. Chem.* 279, 37227–37230.

Please cite this article in press as: Kubo-Murai, M. et al., Protein kinase C $\delta$  binds TIRAP/Mal to participate in TLR signaling, *Mol. Immunol.* (2006), doi:10.1016/j.molimm.2006.11.005

- Mansell, A., Smith, R., Doyle, S.L., Gray, P., Fenner, J.E., Crack, P.J., Nicholson, S.E., Hilton, D.J., O'Neill, L.A., Hertzog, P.J., 2006. Suppressor of cytokine signaling 1 negatively regulates toll-like receptor signaling by mediating Mal degradation. *Nat. Immunol.* 7, 148–155.
- McDermott, E.P., O'Neill, L.A., 2002. Ras participates in the activation of p38 MAPK by interleukin-1 by associating with IRAK, IRAK2, TRAF6, and TAK-1. *J. Biol. Chem.* 277, 7808–7815.
- Monick, M.M., Carter, A.B., Flaherty, D.M., Peterson, M.W., Hunninghake, G.W., 2000. Protein kinase C zeta plays a central role in activation of the p42/44 mitogen-activated protein kinase by endotoxin in alveolar macrophages. *J. Immunol.* 165, 4632–4639.
- Oshiumi, H., Matsumoto, M., Funami, K., Akazawa, T., Seya, T., 2003a. TICAM-1, an adaptor molecule that participates in toll-like receptor 3-mediated interferon-beta induction. *Nat. Immunol.* 4, 161–167.
- Oshiumi, H., Sasai, M., Shida, K., Fujita, T., Matsumoto, M., Seya, T., 2003b. TIR-containing adapter molecule (TICAM)-2, a bridging adapter recruiting to toll-like receptor 4 TICAM-1 that induces interferon-beta. *J. Biol. Chem.* 278, 49751–49762.
- Platten, M., Eitel, K., Wischhusen, J., Dichgans, J., Weller, M., 2003. Involvement of protein kinase Cdelta and extracellular signal-regulated kinase-2 in the suppression of microglial inducible nitric oxide synthase expression by *N*-[3,4-dimethoxycinnamoyl]-anthranilic acid (traniLAST). *Biochem. Pharmacol.* 66, 1263–1270.
- Qian, Y., Commane, M., Ninomiya-Tsuji, J., Matsumoto, K., Li, X., 2001. IRAK-mediated translocation of TRAF6 and TAB2 in the interleukin-1-induced activation of NF-kappa B. *J. Biol. Chem.* 276, 41661–41667.
- Saharinen, P., Ekman, N., Sarvas, K., Parker, P., Alitalo, K., Silvennoinen, O., 1997. The Bmx tyrosine kinase induces activation of the Stat signaling pathway, which is specifically inhibited by protein kinase Cdelta. *Blood* 90, 4341–4353.
- Sanz, L., Diaz-Meco, M.T., Nakano, H., Moscat, J., 2000. The atypical PKC-interacting protein p62 channels NF-kappaB activation by the IL-1-TRAF6 pathway. *Embo. J.* 19, 1576–1586.
- Sasai, M., Oshiumi, H., Matsumoto, M., Inoue, N., Fujita, F., Nakanishi, M., Seya, T., 2005. Cutting Edge: NF-kappaB-activating kinase-associated protein 1 participates in TLR3/Toll-IL-1 homology domain-containing adapter molecule-1-mediated IFN regulatory factor 3 activation. *J. Immunol.* 174, 27–30.
- Sato, S., Sugiyama, M., Yamamoto, M., Watanabe, Y., Kawai, T., Takeda, K., Akira, S., 2003. Toll/IL-1 receptor domain-containing adaptor inducing IFN-beta (TRIF) associates with TNF receptor-associated factor 6 and TANK-binding kinase 1, and activates two distinct transcription factors, NF-kappa B and IFN-regulatory factor-3, in the toll-like receptor signaling. *J. Immunol.* 171, 4304–4310.
- Shinji, H., Akagawa, K.S., Yoshida, T., 1994. LPS induces selective translocation of protein kinase C-beta in LPS-responsive mouse macrophages, but not in LPS-nonresponsive mouse macrophages. *J. Immunol.* 153, 5760–5771.
- Shinohara, H., Yasuda, T., Aiba, Y., Sanjo, H., Hamadate, M., Watarai, H., Sakurai, H., Kurosaki, T., 2005. PKC beta regulates BCR-mediated IKK activation by facilitating the interaction between TAK1 and CARMA1. *J. Exp. Med.* 202, 1423–1431.
- Sommer, K., Guo, B., Pomerantz, J.L., Bandaranayake, A.D., Moreno-Garcia, M.E., Ovechkina, Y.L., Rawlings, D.J., 2005. Phosphorylation of the CARMA1 linker controls NF-kappaB activation. *Immunity* 23, 561–574.
- Wang, Y., Tang, Y., Teng, L., Wu, Y., Zhao, X., Pei, G., 2006. Association of beta-arrestin and TRAF6 negatively regulates Toll-like receptor-interleukin 1 receptor signaling. *Nat. Immunol.* 7, 139–147.
- Wong, B.R., Besser, D., Kim, N., Arron, J.R., Vologodskaya, M., Hanafusa, H., Choi, Y., 1999. TRANCE, a TNF family member, activates Akt/PKB through a signaling complex involving TRAF6 and c-Src. *Mol. Cell.* 4, 1041–1049.
- Xu, Y., Tao, X., Shen, B., Horng, T., Medzhitov, R., Manley, J.L., Tong, L., 2000. Structural basis for signal transduction by the Toll/interleukin-1 receptor domains. *Nature* 408, 111–115.
- Yamamoto, M., Sato, S., Hemmi, H., Uematsu, S., Hoshino, K., Kaisho, T., Takeuchi, O., Takeda, K., Akira, S., 2003. TRAM is specifically involved in the toll-like receptor 4-mediated MyD88-independent signaling pathway. *Nat. Immunol.* 4, 1144–1150.
- Yamamoto, M., Takeda, K., Akira, S., 2004. TIR domain-containing adaptors define the specificity of TLR signaling. *Mol. Immunol.* 40, 861–868.

# Antitumor NK activation induced by the Toll-like receptor 3-TICAM-1 (TRIF) pathway in myeloid dendritic cells

Takashi Akazawa\*, Takashi Ebihara<sup>†</sup>, Manabu Okuno\*\*, Yu Okuda\*\*, Masashi Shingai<sup>†</sup>, Kunio Tsujimura<sup>§</sup>, Toshitada Takahashi<sup>§</sup>, Masahito Ikawa<sup>¶</sup>, Masaru Okabe<sup>¶</sup>, Norimitsu Inoue<sup>||</sup>, Miki Okamoto-Tanaka\*\*, Hiroyoshi Ishizaki\*\*, Jun Miyoshi\*\*, Misako Matsumoto\*<sup>†</sup>, and Tsukasa Seya\*<sup>†,††</sup>

Departments of \*Immunology, <sup>¶</sup>Molecular Genetics, and \*\*Molecular Biology, Osaka Medical Center for Cancer, Nakamichi 1-3-2, Higashinari-ku, Osaka 537-8511, Japan; <sup>†</sup>Department of Microbiology and Immunology, Hokkaido University Graduate School of Medicine, Kita-15, Nishi-7, Kita-ku Sapporo 060-8638, Japan; <sup>§</sup>Department of Molecular Immunology, Nara Institute of Science and Technology, Ikoma, Nara 631-0101, Japan; <sup>||</sup>Division of Immunology, Aichi Cancer Center Research Institute, Nagoya, Aichi 464-8681, Japan; and <sup>¶</sup>Genome Information Research Center, Osaka University, Suita, Osaka 565-0871, Japan

Edited by Tadatsugu Taniguchi, University of Tokyo, Tokyo, Japan, and approved November 4, 2006 (received for review July 17, 2006)

Myeloid dendritic cells (mDCs) recognize and respond to polyI:C, an analog of dsRNA, by endosomal Toll-like receptor (TLR) 3 and cytoplasmic receptors. Natural killer (NK) cells are activated *in vivo* by the administration of polyI:C to mice and *in vitro* are reciprocally activated by mDCs, although the molecular mechanisms are as yet undetermined. Here, we show that the TLR adaptor TICAM-1 (TRIF) participates in mDC-derived antitumor NK activation. In a syngeneic mouse tumor implant model (C57BL/6 vs. B16 melanoma with low H-2 expresser), i.p. administration of polyI:C led to the retardation of tumor growth, an effect relied on by NK activation. This NK-dependent tumor regression did not occur in TICAM-1<sup>-/-</sup> or IFNAR<sup>-/-</sup> mice, whereas a normal NK antitumor response was induced in PKR<sup>-/-</sup>, MyD88<sup>-/-</sup>, IFN- $\beta$ <sup>-/-</sup>, and wild-type mice. IFNAR was a prerequisite for the induction of IFN- $\alpha/\beta$  and TLR3. The lack of TICAM-1 did not affect IFN production but resulted in unresponsiveness to IL-12 production, mDC maturation, and polyI:C-mediated NK-antitumor activity. This NK activation required NK-mDC contact but not IL-12 function in *in vitro* transwell analysis. Implanted tumor growth in IFNAR<sup>-/-</sup> mice was retarded by adoptively transferring polyI:C-treated TICAM-1-positive mDCs but not TICAM-1<sup>-/-</sup> mDCs. Thus, TICAM-1 in mDCs critically facilitated mDC-NK contact and activation of antitumor NK, resulting in the regression of low MHC-expressing tumors.

antitumor immunity | type I interferon | syngenic tumor | implant model | gene-disrupted mice

Enhancing host immunity and increasing tumor antigenicity long have been goals of immunotherapy. Rosenberg *et al.* (1) summarized the results of 440 cancer patients who received a peptide vaccine. The overall objective response rate for all vaccine treatments was just 2.6% (1). Although their criteria for clinical objective response were strict, the results clearly reflect a limited effectiveness of the sole peptide vaccine therapy approach. Tumor cells often have diminished MHC class I (2), thereby circumventing the host immune surveillance system. They suggested that further technical exploration would be required, including additional manipulations of the vaccination procedure to establish effective tumor immunotherapy. Adjuvants are known to serve largely as ligands for Toll-like receptors (TLRs) (3, 4) and have the potential to compensate for the weakness of the peptide vaccine therapy. We have elucidated some of the roles of adjuvant in immunotherapy (5).

CTL and natural killer (NK) cells are two major cellular effectors against tumors. CTL mainly eliminate tumors with high levels of MHC class I proteins, whereas NK cells target tumors with low MHC levels. We have studied the profiles of effector induction in myeloid dendritic cells (mDCs) stimulated with adjuvants (5). In human and mouse, the bacillus Calmette–Guérin-cell-wall skeleton

acts as a TLR2/4 agonist and induces mDC maturation followed by tumor-specific CTL in a syngeneic tumor implantation model if the tumors express MHC class I (5). Tumor regression and CTL induction largely relied on the MyD88 adapter-dependent pathway of TLR (5). Exogenously added tumor antigen (Ag) and adjuvant induce the mDCs cross-priming, which is required for MHC class I-mediated Ag presentation and CTL induction (6, 7). However, an MHC-negative population of the implant tumor survives to proliferate even after CTL induction. NK cells barely are activated in wild-type mice via the TLR2/4-MyD88 responses (5). Thus, MyD88-independent cellular responses are crucial in NK-mediated tumor cytotoxicity.

The TLR3 agonist polyI:C and TLR3 signaling in mDCs are able to regress tumors (6). TLR3 links TICAM-1 (or TRIF) in the cytoplasmic domain TIR (Toll-IL-1R homology domain) for signal transmission (8, 9). This adapter is unique in possessing two arrays of signals that activate two transcription factors, NF- $\kappa$ B and interferon (IFN) regulatory factor-3 (8–10). The latter is a strong inducer of type I IFN, particularly IFN- $\beta$  (10–12). Recent reports suggest an important role for type I IFN in p53 induction (13) and cancer immunoediting (14). Type I IFN has been reported to be an inducer of various NK functions *in vitro* (15). Amplification of type I IFN production by IFNAR governs the expression of a number of IFN-inducible genes (16). These genes may be crucial for the functional modulation of mDCs.

mDCs and NK cells reciprocally activate one another during the immune response (15, 17). Several *in vitro* studies have shown that direct cell-cell contact as well as cytokines, including IFN- $\gamma$ , IL-12, and TNF- $\alpha$ , are involved in NK activation by mDCs (15, 17, 18). However, *in vivo* the molecular mechanism for reciprocal mDC maturation and NK activation has not been elucidated.

Here, we have investigated the mechanism whereby exogenously administered polyI:C induces tumor regression in gene-disrupted mice. We noticed that the retardation in the growth of MHC-negative tumors largely depended on the NK activity induced by polyI:C-stimulated mDCs. Using TICAM-1 (TRIF)<sup>-/-</sup> C57BL/6 mice [supporting information (SI) Fig. 7]

Author contributions: T.A., M.M., and T.S. designed research; T.A., T.E., M. Okuno, Y.O., and M.S. performed research; K.T., T.T., M.I., M. Okabe, M.O.-T., H.I., and J.M. contributed new reagents/analytic tools; N.I., M.M., and T.S. analyzed data; and T.S. wrote the paper.

The authors declare no conflict of interest.

This article is a PNAS direct submission.

<sup>††</sup>To whom correspondence should be addressed. E-mail: seya-tu@med.hokudai.ac.jp.

Abbreviations: KO, knockout; mDC, myeloid dendritic cell; NK, natural killer; TLR, Toll-like receptor.

This article contains supporting information online at [www.pnas.org/cgi/content/full/0605978104/DC1](http://www.pnas.org/cgi/content/full/0605978104/DC1).

© 2006 by The National Academy of Sciences of the USA



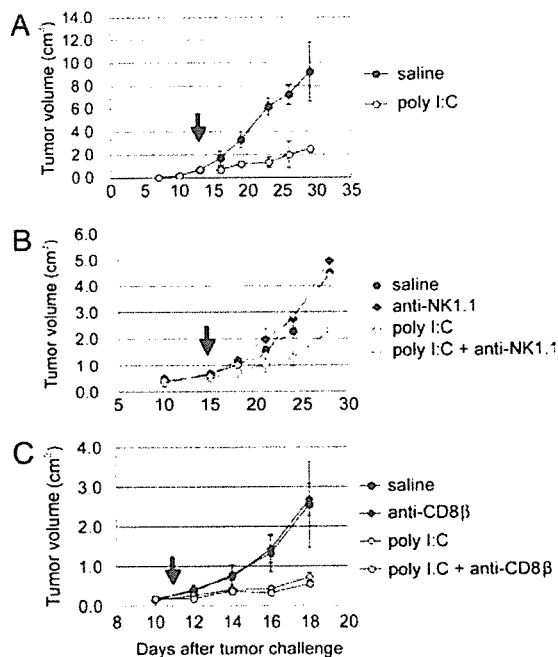


**Fig. 1.** PolyI:C induces NK-mediated MHC class I-negative tumor regression. (A) Establishment of tumor-implantation model for evaluation of polyI:C antitumor activity. PolyI:C (250  $\mu$ g i.p. injected twice a week) caused antitumor effect on B16D8 cells (SI Fig. 8) implanted into C57BL/6 mice. Arrow indicates the start point of polyI:C treatment (tumor average size  $>0.8$  cm $^3$ ). (B and C) NK is an effector for poly(I:C)-mediated antitumor activity. Mice were challenged with B16D8 cells and i.p. injected with anti-NK1.1 (B) or anti-CD8 $\beta$  (C) ascites according to the schedule of polyI:C treatment (see *Materials and Methods*). Antibody and polyI:C treatment was repeated twice a week from day 10. One of the two similar experiments is shown.

and a syngeneic tumor implant model, this NK activation was found to depend on direct contact of NK cells to mDCs, where NK activation is controlled by the TICAM-1 pathway of TLR in mDCs.

## Results

**Retardation of Tumor Growth by NK Cells in polyI:C-Treated Mice.** PolyI:C is reported to induce type I IFN *in vivo* in mice and *in vitro* in mDCs (19, 20). Using a C57BL/6-B16 syngeneic tumor-implant model, we evaluated the antitumor activity of polyI:C, which was injected i.p. twice a week (Fig. 1A). Suppression of tumor growth, determined as reported in ref. 5, was observed in the group that received polyI:C compared with the saline-treated group. The retardation of tumor growth appeared to depend on polyI:C treatment but not on the level of MHC class I or a direct effect (such as apoptosis) on B16 cells (SI Figs. 8 and 9).

PolyI:C-mediated suppression of tumor growth was terminated when NK activity in mice was blocked by an injection of NK1.1 Ab (Fig. 1B) or asialo-GM1 Ab (data not shown). Thus, the polyI:C-mediated tumor suppression largely relies on the effector NK cells. Similar experiments by using another model (BALB/c vs. CT-26) and asialo-GM1 Ab confirmed the results obtained with the C57BL/6 vs. B16 model (data not shown).

Similar experiments by using the syngeneic mouse model were performed with CD8-eliminating Ab (Fig. 1C). Suppression of B16 tumor growth was not significantly changed by the treatment of mice with anti-CD8 Ab. CD8 $^+$  CTL-mediated tumor suppression is minimal, if any, in this model.

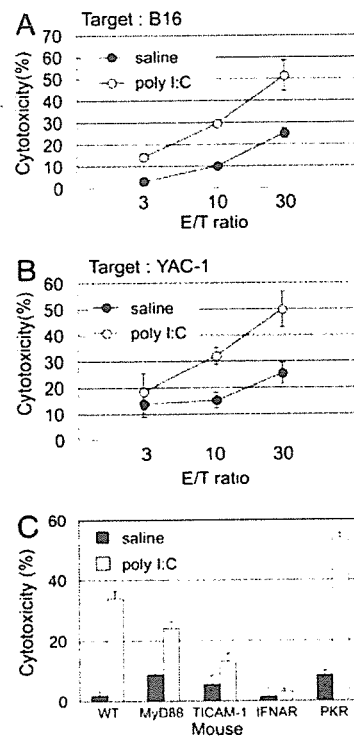


**Fig. 2.** Antitumor NK cells isolated from polyI:C-injected C57BL/6 mice. (A) *In vitro* B16 cytotoxicity by splenic NK cells of polyI:C-treated mice. C57BL/6 mice were administered with polyI:C (or control saline only) i.p. After 18 h, NK cells were isolated with MACS-negative selection beads and NK cytotoxicity against B16 cells was measured by  $^{51}$ Cr release assay. (B) YAC-1 cytotoxicity of splenocytes was tested as in A. YAC-1 is known to be targets for NK. (C) NK activation depends on TICAM-1 and IFNAR. YAC-1 cytotoxicity of splenocytes from gene-disrupted mice stimulated with polyI:C. Indicated gene-disrupted mice were treated with polyI:C. After 18 h, splenocytes were prepared and their cytotoxicity against YAC-1 was measured by  $^{51}$ Cr release assay. NK activation by polyI:C was impaired in splenocytes derived from IFNAR $^{-/-}$  or TICAM-1 $^{-/-}$  mice. Effector-to-target cell ratio (E/T ratio) = 100. One of the three independent experiments is shown.

**TICAM-1 and IFNAR Participate in NK Activation in Mice.** We then assessed the tumor cytotoxicity of NK cells isolated from polyI:C-administered C57BL/6 mice. PolyI:C was administered i.p. to mice, and the spleen cells were collected as a source of NK cells. To eliminate contaminating NKT cells, negative selection was performed to isolate NK cells by using MACS beads. NK cells efficiently expressed tumoricidal activity against the same lot of B16 melanoma cells (Fig. 2A). YAC-1 (an NK target) cells were killed in a fashion similar to B16 cells (Fig. 2B), supporting the view that NK is the effector. B16 and YAC-1 were used to measure the cytotoxicity of spleen cells collected from the indicated polyI:C-treated knockout (KO) mice (Fig. 2C). A significant decrease of cytotoxicity was observed in spleen cells prepared from IFNAR $^{-/-}$  or TICAM-1 $^{-/-}$  mice. The polyI:C-mediated YAC-1 cytotoxicity was reduced only slightly in spleen cells of MyD88 $^{-/-}$  mice. NK-mediated cytotoxicity increased in cells from PKR $^{-/-}$  mice. Similar results were obtained with B16 cells (data not shown).

To further confirm the results of Fig. 2C, B16 cells were implanted and tumor growth was followed *in vivo* in these KO mice. Retardation of B16 tumor growth by polyI:C was observed in MyD88 $^{-/-}$ , IFN- $\beta$  $^{-/-}$ , and PKR $^{-/-}$  mice at a level comparable to the control wild-type mice (Fig. 3). The antitumor activity of

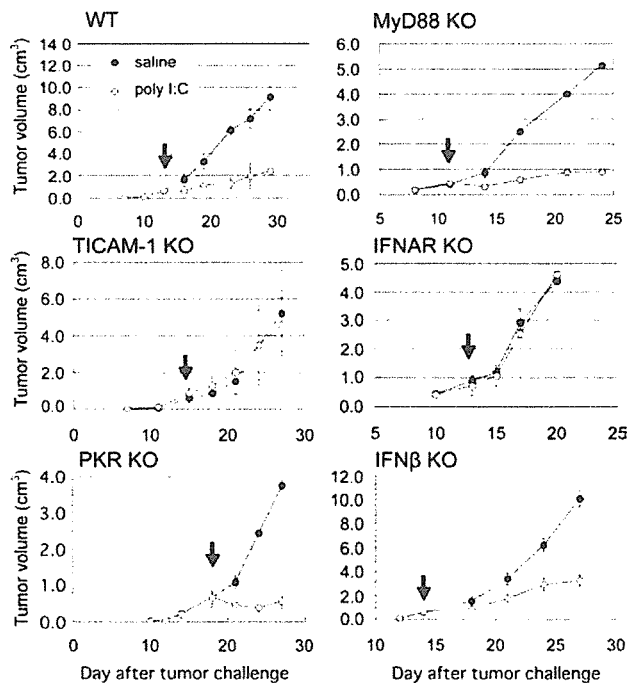


**Fig. 3.** Antitumor activity of PolyI:C depends on TICAM-1 and IFNAR *in vivo*. Antitumor effect of polyI:C on various KO mice were evaluated by using *in vivo* mouse tumor implant model. B16 tumor cells were inoculated on day 0. Arrow indicates the start point of polyI:C administration. Each point represents tumor size average  $\pm$  SE ( $n = 4-6$ ). The disrupted genes in mice are shown over the graphs.

polyI:C diminished in TICAM-1<sup>-/-</sup> or IFNAR<sup>-/-</sup> mice (Fig. 3). Tumor regression by polyI:C was not affected by depletion of IFN- $\beta$ , suggesting the participation of other IFNs (especially IFN- $\alpha$ ) in the IFNAR-mediated antitumor response. These results infer that the antitumor activity by polyI:C is elicited through TICAM-1 and/or IFNAR in these mice. In the absence of IFNAR, no TLR3 was expressed by stimulation with polyI:C in mDCs (SI Fig. 10); therefore, the TLR3-TICAM-1 pathway does not function in IFNAR<sup>-/-</sup> mice. Taken together, the final effector for tumor killing is evidently NK cells activated in association with TLR3-TICAM-1 in this mouse tumor-implant model (Figs. 1 B and C and 3).

**Mechanisms of NK Activation by polyI:C-Stimulated mDCs.** The TICAM-1-dependent NK activation in polyI:C-treated mice was unexpected because polyI:C functions through multiple pattern-recognition receptors, i.e., PKR, RIG-I, and MDA5, in addition to TLR3 (21-23). All these receptors are induced by IFN- $\alpha/\beta$  in mDCs to recognize polyI:C *in vitro* (20). Although RIG-I and MDA5 were normally induced in TICAM-1<sup>-/-</sup> mDCs (SI Fig. 11), polyI:C-mediated NK activation was abolished in TICAM-1<sup>-/-</sup> mice (Fig. 3). We then aimed at clarifying the point that TICAM-1 in mDCs is responsible for the *in vivo* and *in vitro* antitumor NK activation by polyI:C.

TICAM-1 in mDCs participates in NK activation because adoptive transfer of mDCs with TICAM-1 overexpression (SI Fig. 12) also retarded tumor growth in wild-type mice (Fig. 4A). *In vitro* cytotoxic assay was performed with B16 cells and NK cells treated with TICAM-1-transduced mDCs (Fig. 4B). B16 cells were damaged by NK cells cocultured with polyI:C-treated mDCs, and to a lesser extent, with TICAM-1-transduced mDCs. Thus, mDCs expressing TLR3-TICAM-1 contribute to antitumor NK activation.

We next tested whether IFNAR in mDCs or other cells is

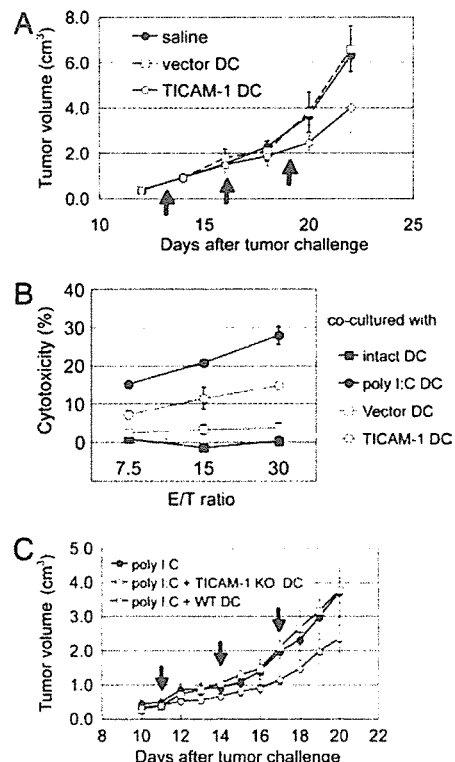


**Fig. 4.** TICAM-1 in mDCs is essential for antitumor activity of polyI:C. (A) Adoptive transfer of TICAM-1-transduced mDCs confers tumor growth suppression in mice. The lentiviral system was used for gene transfection into mDCs (SI Fig. 12). mDCs were prepared from bone marrow cells and transfected with TICAM-1 (TICAM-1 DC) or empty vector (vector DC). Wild-type mice were implanted with B16 cells on day 0. On day 12, 16, and 19, the mice with tumor burden were i.p. injected with TICAM-1-expressing mDCs ( $1 \times 10^6$  cells). Retardation of tumor growth was measured in the mice of control, with vector-containing mDCs or with TICAM-1-expressing mDCs. One of the three independent experiments is shown. (B) B16 killing by NK cells cocultured with mDCs. TICAM-1-expressing mDCs (TICAM-1 DC) and vector DC were prepared as in A. Poly I:C-stimulated mDCs (polyI:C DC) were prepared by incubation of mDCs with poly I:C for 4 h. The mDCs were cocultured with NK cells (DC:NK = 1:2) for 24 h. NK cytotoxicity against B16 was measured by <sup>51</sup>Cr release assay. (C) TICAM-1 in mDCs is required for polyI:C-mediated tumor regression. mDCs were prepared from wild-type and TICAM-1 KO mice. mDCs ( $3 \times 10^6$  cells) either from wild-type (WT DC) or TICAM-1 KO mice (TICAM-1 KO DC) and polyI:C (250  $\mu$ g) were injected into the peritoneal cavity of IFNAR<sup>-/-</sup> mice, which had the tumor burden. Growth retardation of implanted tumor in response to polyI:C was measured in the mDC-injected mice. The arrows indicate the time points at which the mDCs were administered.

important for mDC-mediated NK activation. IFNAR is distributed across mDCs and lymphocytes, including NK cells. The IFNAR<sup>-/-</sup> mice essentially failed to respond to polyI:C for tumor regression. When IFNAR-positive mDCs were transferred into IFNAR<sup>-/-</sup> mice, polyI:C-mediated antitumor NK activation was recovered in the IFNAR<sup>-/-</sup> mice (Fig. 4C). In contrast, no recovery of polyI:C-mediated tumor regression was observed by supplementing TICAM-1<sup>-/-</sup> mDCs into IFNAR<sup>-/-</sup> mice with the tumor burden (Fig. 4C). Thus, mDCs lead to tumoricidal NK activation in response to polyI:C *in vivo* and *in vitro*, where mDC TICAM-1 and IFNAR actively are involved.

The mechanism whereby TICAM-1 induces NK activation then was analyzed. Rae-1 proteins are up-regulated by TLR stimuli on murine macrophages and serve as ligands for NKG2D on NK cells (24). We checked the level of Rae-1 in mDCs. The Rae-1 level was not altered in response to polyI:C stimulation (SI Fig. 10). Next, we

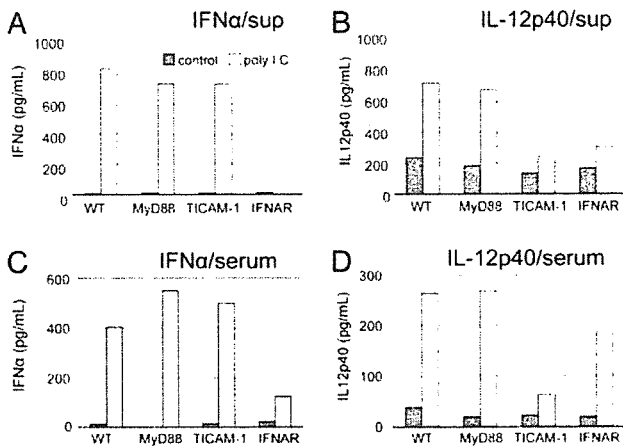


**Fig. 5.** Production of IFN- $\alpha$  and IL12p40 in response to polyI:C stimulation *in vivo* and *in vitro*. The concentrations of IFN- $\alpha$  and IL12p40 in cultured sup (A and B) of mDCs and in mouse serum (C and D) were determined by ELISA. mDCs were prepared from each KO mice and stimulated with 50  $\mu$ g of polyI:C. After 24 h, culture supernatants were collected and the levels of cytokines (A and B) were measured. In other experiments, each indicated KO mouse was i.p. injected with polyI:C. After 16 h, blood was directly drawn from heart and clotted to collect serum (C and D). It is notable that IFNAR<sup>-/-</sup> mice failed to produce IFN- $\alpha$  *in vivo* and *in vitro*, but TICAM-1<sup>-/-</sup> mice retained IFN-producing capacity. Gray bars, controls with no stimulation; white bars, cells/mice stimulated with polyI:C. Figure represents one of four experiments.

measured the cytokine levels in the culture supernatant (sup) of polyI:C-stimulated mDCs prepared from gene-disrupted mice (Fig. 5A and B). IFNAR<sup>-/-</sup> mDCs did not release IFN- $\alpha$ , whereas TICAM-1<sup>-/-</sup> mDCs and conventional (prepared from wild-type mice) and MyD88<sup>-/-</sup> mDCs released it by stimulation with polyI:C (Fig. 5A). There was only marginal up-regulation of IL-12 p40 (Fig. 5B) or mDC maturation (SI Fig. 13) by polyI:C in TICAM-1<sup>-/-</sup> and IFNAR<sup>-/-</sup> mDCs. However, mDCs are not merely a cell type producing IL-12 and type I IFN, and these cytokine profiles were somewhat discrepant in the serum of polyI:C-treated KO mice (Fig. 5C and D). Furthermore, polyI:C-mediated tumor regression was not abolished by functional blockade of IL-12 in the B16 tumor implant model (SI Fig. 14), nor was the *in vitro* B16 tumor killing by NK cells cocultured with polyI:C-primed mDCs cancelled by the addition of IL-12-neutralizing Ab (Fig. 6A). The IL-12/IFN- $\alpha/\beta$  profiles in the serum are not consistent with the degrees of NK activation.

B16 killing due to NK cells activated by polyI:C-primed mDCs was impaired if spleen NK cells were cultured with polyI:C-primed mDCs in the transwell (Fig. 6B), suggesting that tumoricidal activity NK cells acquire via mDCs is attributable largely to cell-cell contact.

RIG-I and MDA5 as well as TLR3 and IFN- $\alpha/\beta$  are IFN-inducible genes that were up-regulated in the response of mDCs to polyI:C within 6 h (SI Fig. 11). The up-regulation was impaired in IFNAR<sup>-/-</sup> mice but not TICAM-1<sup>-/-</sup> mice (SI Fig. 11). We tested whether TICAM-1<sup>-/-</sup> mDCs stimulated with polyI:C still retain the activity to induce antitumor NK cells (Fig. 6C). Only weak antitumor NK activity was detected when the spleen NK cells were preincubated with TICAM-1<sup>-/-</sup> mDCs. Costimulator CD86 up-regulation in response to polyI:C also was impaired in the mDCs prepared from TICAM-1<sup>-/-</sup> as well as IFNAR<sup>-/-</sup> mice (SI Fig. 13). Thus, NK cell-binding molecules, rather than cytokines, are induced in mDCs through the TLR3-TICAM-1 pathway in response to exogenic dsRNA stimuli, which may explain the functional link between mDC TICAM-1 and NK activation.

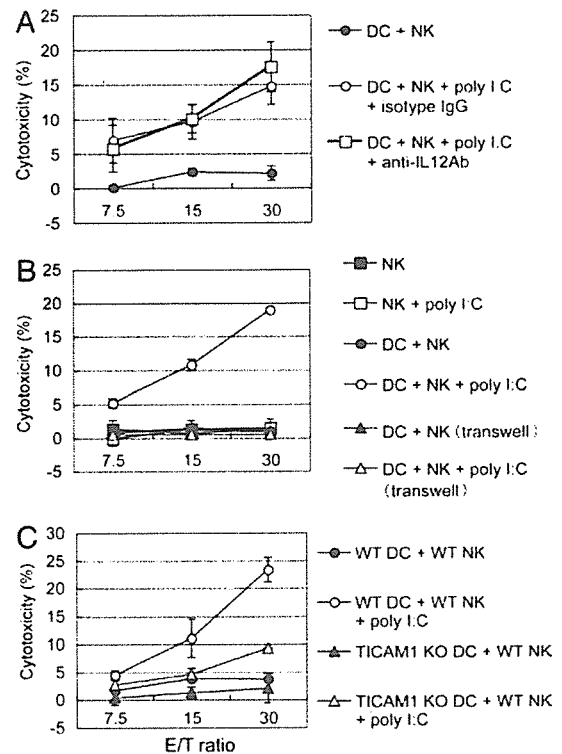


**Fig. 6.** mDCs activate NK cells via cell-cell contact, which depends on the TICAM-1 pathway. mDCs prepared from wild-type or TICAM-1 KO mice were incubated with polyI:C for 24 h, and NK cells were added to the culture at an mDC/NK ratio of 1:2. After 24 h, NK cells were incubated with B16 cells for 5 h at the indicated effector-to-target cell ratio (E/T ratio). Cytotoxicity of NK against B16 cells was examined by <sup>51</sup>Cr release assay. (A and B) NK cells were cocultured with mDCs in the presence of 5  $\mu$ g/ml anti-IL12 antibody (A) or in the transwell system (B). (C) NK cells cocultured with mDCs derived from TICAM-1 KO mice.

## Discussion

Here, we have demonstrated that TICAM-1 and IFNAR are involved in polyI:C-mediated maturation of mDCs and the generation of antitumor NK activity *in vivo* by using mouse models. Adoptive transfer of TICAM-1-positive mDCs but not TICAM-1-deficient mDCs exerted polyI:C-dependent suppression of tumor growth in IFNAR<sup>-/-</sup> mice (Fig. 4), suggesting that a unique TICAM-1-dependent response occurs in mDCs that elicits antitumor immunity. This effector is NK, a finding that is reinforced by the fact that the polyI:C-dependent tumor regression is abrogated largely by the administration of NK1.1 or asialoGM1 Ab. Thus, the NK-activating mDC subset is induced through the TICAM-1 pathway by the administration of polyI:C.

NK cells and mDCs are activated reciprocally via cytokines/IFNs and/or cell-to-cell contact (17). The molecular mechanism by which mDCs activate NK has not been clearly addressed. This study demonstrates that the TICAM-1 pathway in mDCs serves to modulate mDCs to have NK-activating properties leading to the induction of tumoricidal NK activation.

Whereas TICAM-1 and IFNAR are not IFN-inducible, RIG-I, MDA5, TLR3, and IFN- $\alpha$  are IFN-inducible genes. They are rapidly up-regulated in response to polyI:C (SI Fig. 11). Thus, IFNAR is an indispensable factor for inducing TLR3 to complete the TLR3-TICAM-1 pathway and stimulate RIG-I/MDA5 to amplify IFN- $\alpha/\beta$  production. However, exogenously added IFN- $\alpha/\beta$  does not elicit NK-activating mDCs. Furthermore, adoptive transfer of TICAM-1-positive mDCs into IFNAR<sup>-/-</sup>

mice with a tumor burden elicits an antitumor response. Thus, the type I IFN robustly produced by lymphocyte IFNAR barely participates in the elicitation of antitumor NK activity. Although MDA5 and RIG-I are normally induced by polyI:C in TICAM-1<sup>-/-</sup> mice with the ability to induce type I IFN (20, 23), mDCs in TICAM-1<sup>-/-</sup> mice have lost NK-activating activity in response to polyI:C. In fact, *in vitro* NK-mediated tumor-killing activity is minimally induced via coculture of NK cells with polyI:C-treated TICAM-1<sup>-/-</sup> mDCs (Fig. 6C). Cell-cell contact rather than IL-12 or IFN- $\alpha/\beta$  is closely associated with provoking NK-mediated tumor cytotoxicity (Fig. 6B). Hence, the NK-activating property depends only partly on cytokines or RIG-I/MDA5 but is rooted in the factors secondary to TICAM-1 in mDCs.

IFN- $\alpha/\beta$  and/or IL-12 p40 have been reported to be associated with NK activation *in vitro* (25). A primary role of pDCs in IFN- $\alpha/\beta$  (26) and NK activation (25) has been reported. However, this is not the case in *in vivo* NK-mediated tumor suppression. The most likely route for the activation of tumoricidal NK cells is in mDCs consisting of endosomal TLR3 and TICAM-1. The identification of TICAM-1-inducing NK-activating molecules in mDCs will foster an elucidation of the mechanism by which mDCs take on the NK-activating phenotype.

Moderately successful targeting of TLR3 by dsRNA in breast cancer has been reported with certain side effects (27). These investigations have suggested the TLR3 on tumor cells is a specific trigger of apoptosis signaling. Thus, the main focus in those studies was on polyI:C as an inducer of apoptosis in tumor cells (28). Other *in vitro* studies have suggested that the TLR3 pathway in mDCs is involved in cross-priming and CTL induction (6, 29). In this study, we show that the TICAM-1 pathway in mDCs induces mDC maturation that, in turn, directs NK activation. dsRNA acts on mDCs and tumor cells and in mDCs has multiple targets, resulting in the exerting of CTL induction and/or NK activation, both of which are pivotal in antitumor immunity.

Ultimately, polyI:C-mediated NK activation can be assigned to certain NK-activating ligands induced through the TLR3-TICAM-1 pathway in mDCs. Target recognition by NK is determined by the balance of NK-activating and -inhibitory receptors (30). These receptor ligands are variably expressed on mDCs (31) as well as tumor cells (32). Identification of the NK-activating molecules inducible on mDCs by dsRNA should lead to novel antitumor strategies against a variety of tumors.

## Materials and Methods

**Mice, Cells, and Reagents.** TICAM-1<sup>-/-</sup> mice were backcrossed more than eight times to adapt the C57BL/6 background. PKR<sup>-/-</sup> (33), TLR3<sup>-/-</sup> (19), MyD88<sup>-/-</sup> (34), IFN- $\beta$ <sup>-/-</sup> (35), and IFNAR<sup>-/-</sup> mice (36) were provided by T. Taniguchi (University of Tokyo, Tokyo, Japan) and S. Akira (Osaka University). All of the mice were maintained under specific pathogen-free conditions in the animal facility of the Osaka Medical Center and the Graduate School of Medicine Hokkaido University. They were backcrossed with C57BL/6 mice 8 to 10 times before use. Animal experiments were performed according to the guidelines set by the animal safety center, Japan.

B16D8 cell line was established in our laboratory as a subline of B16 melanoma (37). This subline was characterized by its low or virtually no metastatic properties when injected s.c. into syngeneic C57BL/6 mice (37). The mouse YAC-1 (BALB/c origin) cell line was provided by Sumitomo (Osaka, Japan), as described in ref. 32. These cell lines were cultured in RPMI medium 1640/10% FCS. Mouse NK cell was isolated with MACS Beads (Miltenyi Biotec, Auburn, CA). Bone marrow-derived mDCs were prepared as reported in ref. 38 with minor modifications.

**Tumor Challenge and polyI:C Treatment.** Mice were shaved at the flank and injected s.c. with 300  $\mu$ l of  $6 \times 10^5$  syngeneic B16D8 melanoma cells in PBS. After 1 week, tumor volumes were

measured at regular intervals by using a caliper. Tumor volume was calculated by using the formula: Tumor volume (cm<sup>3</sup>) = (long diameter)  $\times$  (short diameter)  $\times$  (thickness)  $\times$  0.4. PolyI:C was injected i.p. at a concentration of 250  $\mu$ g per head. The treatments were started on day 10–14 (when average of tumor volume reached at 0.5–0.8 cm<sup>3</sup>) and were repeated twice a week.

To deplete CD8<sup>+</sup> T cells and NK cells *in vivo*, mice were i.p. injected with hybridoma ascites of anti-CD8 $\beta$  mAb and anti-NK1.1 mAb (39). All doses of antibodies and treatment regimens were determined in preliminary studies by using the same lots of antibodies used for the experiments. Treatment was confirmed to deplete completely the desired cell populations for the entire duration of the study.

**TICAM-1 Gene-Transfected mDC Therapy.** mDCs were transfected with mouse TICAM-1 cDNA by Lenti-viral transfection system (Invitrogen, Carlsbad, CA). The preparation and propagation of lentivirus were performed as follows (31). A sequence of hrGFP with the multicloning site with hrGFP was cloned from pIRES-hrGFP-1a vector (Stratagene, La Jolla, CA) and placed into the cloning site of pLenti6/V5-D-TOPO vector (Invitrogen) by TOPO-cloning system to add optimal restriction enzyme site to the 3' terminal end of the target gene. This vector was named as pLenti-IRES-hrGFP. We used this empty vector as control. More than 50% of mDCs were GFP-positive after treatment with pLenti-IRES-hrGFP (data not shown).

Mouse TICAM-1 cDNA was cloned as described in ref. 4. In most experiments, a cDNA encoding the N-terminal region of TICAM-1 (1–550 aa) (40) was used instead of the full-length TICAM-1 cDNA, because the full-length TICAM-1 expression led to cell apoptosis within 8 h after transfection. The cDNAs were subcloned and sequenced for confirmation. The cDNAs were ligated into pLenti-IRES-hrGFP vector. The virus dose was determined so as to reach 50% GFP expression in mDCs 36 h after infection (31). Transfection efficiency was checked by using mDCs. Briefly, percent GFP-positive cells was estimated by flow cytometry or counting the cells under illumination of a fluorescence microscope as reported in ref. 41. Virus particles were prepared for transfection according to the manufacturer's protocol.

**Assessment of NK Cytolytic Activity.** Cytolytic activity of splenocytes and purified NK cells derived from polyI:C-treated mice was determined by <sup>51</sup>Cr-release assay. Mice were i.p. injected with 250  $\mu$ g of polyI:C. After 16 h, mice were killed and splenocytes were isolated by using Lympholyte-M. NK cells were purified with MACS-negative selection beads. Target cells were labeled with <sup>51</sup>Cr for 3 h at 37°C, then washed and coincubated with effector cells at the indicated lymphocyte-to-target cell ratio in V-bottom 96-well plates in a total volume of 200  $\mu$ l of RPMI medium 1640. Cytotoxicity was determined by measuring the <sup>51</sup>Cr radioactivity released in 100  $\mu$ l of the supernatant harvested from the plate after 8 h of incubation at 37°C (32). The percentage of specific lysis was calculated by using the formula: %Specific lysis = [(experimental release – spontaneous release)/(total release – spontaneous release)]  $\times$  100.

**Supporting Information.** For additional details, see *SI Materials and Methods* and SI Table 1.

We thank Dr. K. Toyoshima (RIKEN, Yokohama, Japan) for organizing this project, the laboratory members for invaluable discussions, Drs. T. Taniguchi (University of Tokyo) and S. Akira (Osaka University) for providing gene-disrupted mice, and Dr. Boru (Pacific Edit) for reviewing this manuscript. This work was supported in part by CREST and Japan Science and Technology Corporation (JST), Grants-in-Aids from the Ministry of Education, Science, and Culture (Specified Project for Advanced Research) and the Hepatitis C Virus project in National Institutes of Health of Japan, and by the Naito Memorial Foundation, Uehara Memorial Foundation, Mitsubishi Foundation, and Takeda Foundation.

1. Rosenberg SA, Yang JC, Restifo NP (2004) *Nat Med* 10:909–915.
2. Seliger B, Mæurer MJ, Ferrone S (1997) *Immunol Today* 18:292–299.
3. Seya T, Akazawa T, Matsumoto M, Begum NA, Azuma I, Toyoshima K (2002) *Anticancer Res* 23:4369–4376.
4. Medzhitov R, Janeway CA, Jr (1997) *Cell* 91:295–298.
5. Akazawa T, Masuda H, Sacki Y, Matsumoto M, Takeda K, Akira S, Azuma I, Toyoshima K, Seya T (2004) *Cancer Res* 64:757–764.
6. Schulz O, Diebold SS, Chen M, Naslund TI, Nolte MA, Alexopoulou L, Azuma YT, Flavell RA, Liljestrom P, Reis e Sousa C (2005) *Nature* 433:887–892.
7. Datta SK, Redecke V, Prilliman KR, Takabayashi K, Corr M, Tallant T, DiDonato J, Dziarski R, Akira S, Schoenberger SP, Raz E (2003) *J Immunol* 170:4102–4110.
8. Oshiumi H, Matsumoto M, Funami K, Akazawa T, Seya T (2003) *Nat Immunol* 4:161–167.
9. Yamamoto M, Sato S, Hemmi H, Hoshino K, Kaisho T, Sanjo H, Takeuchi O, Sugiyama M, Okabe M, Takeda K, Akira S (2003) *Science* 301:640–643.
10. Fitzgerald KA, McWhirter SM, Faia KL, Rowe DC, Latz E, Golenbock DT, Coyle AJ, Liao SM, Maniatis T (2003) *Nat Immunol* 4:491–496.
11. Mori M, Yoneyama M, Ito T, Takahashi K, Inagaki F, Fujita T (2004) *J Biol Chem* 279:9698–9702.
12. tenOever BR, Servant MJ, Grandvaux N, Lin R, Hiscott J (2002) *J Virol* 76:3659–3669.
13. Takaoka A, Yanai H, Kondo S, Duncan G, Negishi H, Mizutani T, Kano S, Honda K, Ohba Y, Mak TW, Taniguchi T (2005) *Nature* 434:243–249.
14. Dunn GP, Bruce AT, Sheehan KC, Shankaran V, Uppaluri R, Bui JD, Diamond MS, Koebel CM, Arthur C, White JM, Schreiber RD (2005) *Nat Immunol* 6:722–729.
15. Hamerman JA, Ogasawara K, Lanier LL (2005) *Curr Opin Immunol* 17:29–35.
16. Taniguchi T, Takaoka A (2002) *Curr Opin Immunol* 14:111–116.
17. Fernandez NC, Lozier A, Flament C, Ricciardi-Castagnoli P, Bellet D, Suter M, Perricaudet M, Tursz T, Maraskovsky E, Zitvogel L (1999) *Nat Med* 5:405–411.
18. Gerosa F, Baldani-Guerra B, Nisii C, Marchesini V, Carra G, Trinchieri G (2002) *J Exp Med* 195:327–333.
19. Honda K, Sakaguchi S, Nakajima C, Watanabe A, Yanai H, Matsumoto M, Ohteki T, Kaisho T, Takaoka A, Akira S, et al. (2003) *Proc Natl Acad Sci USA* 100:10872–10877.
20. Kato H, Takeuchi O, Sato S, Yoneyama M, Yamamoto M, Matsui K, Uematsu S, Jung A, Kawai T, Ishii KJ, et al. (2006) *Nature* 441:101–105.
21. Yang YL, Reis LF, Pavlovic J, Aguzzi A, Schafer R, Kumar A, Williams BR, Aguet M, Weissmann C (1995) *EMBO J* 14:6095–6106.
22. Yoneyama M, Kikuchi M, Natsukawa T, Shinobu N, Imaizumi T, Miyagishi M, Taira K, Akira S, Fujita T (2004) *Nat Immunol* 5:730–737.
23. Gitlin L, Barchet W, Gilfillan S, Cella M, Beutler B, Flavell RA, Diamond MS, Colonna M (2006) *Proc Natl Acad Sci USA* 103:8459–8464.
24. Hamerman JA, Ogasawara K, Lanier LL (2004) *J Immunol* 172:2001–2005.
25. Degli-Esposti MA, Smyth MJ (2005) *Nat Rev Immunol* 5:112–124.
26. Honda K, Yanai H, Negishi H, Asagiri M, Sato M, Mizutani T, Shimada N, Ohba Y, Takaoka A, Yoshida N, Taniguchi T (2005) *Nature* 434:772–777.
27. Khan AL, Richardson S, Drew J, Larsen F, Campbell M, Heys SD, Ah-Sec AK, Eremin O (1995) *Surgery* 118:531–538.
28. Salaun B, Coste I, Rissoan MC, Lebecque SJ, Renno T (2006) *J Immunol* 176:4894–4901.
29. Iwasaki A, Medzhitov R (2004) *Nat Immunol* 5:987–995.
30. Cerwenka A, Lanier LL (2001) *Nat Rev Immunol* 1:41–49.
31. Dull T, Zufferey R, Kelly M, Mandel RJ, Nguyen M, Trono D, Naldini L (1998) *J Virol* 72:8463–8471.
32. Masuda H, Sacki Y, Nomura M, Hirahashi T, Matsumoto M, Ui M, Lanier LL, Seya T (2002) *Biochem Biophys Res Commun* 290:140–145.
33. Mailliard RB, Son YI, Redlinger R, Coates PT, Giermasz A, Morel PA, Storkus WJ, Kalinski P (2003) *J Immunol* 171:2366–2373.
34. Adachi O, Kawai T, Takeda K, Matsumoto M, Tsutsui H, Sakagami M, Nakanishi K, Akira S (1998) *Immunity* 9:143–154.
35. Takaoka A, Mitani Y, Sucmori H, Sato M, Yokochi T, Noguchi S, Tanaka N, Taniguchi T (2000) *Science* 288:2357–2360.
36. Muller U, Steinhoff U, Reis LF, Hemmi S, Pavlovic J, Zinkernagel RM, Aguet M (1994) *Science* 264:1918–1921.
37. Tanaka H, Mori Y, Ishii H, Akedo H (1988) *Cancer Res* 48:1456–1459.
38. Inaba K, Pack M, Inaba M, Sakuta H, Isdell F, Steinman RM (1997) *J Exp Med* 186:665–672.
39. Uno T, Takeda K, Kojima Y, Yoshizawa H, Akiba H, Mittler RS, Gejyo F, Okumura K, Yagita H, Smyth MJ (2006) *Nat Med* 12:693–698.
40. Oshiumi H, Sasai M, Shida K, Fujita T, Matsumoto M, Seya T (2003) *J Biol Chem* 278:49751–49762.
41. Shingai M, Inoue N, Okabe M, Akazawa T, Miyamoto Y, Ayata M, Honda K, Kurita-Taniguchi M, Matsumoto M, Ogura H, et al. (2005) *J Immunol* 175:3252–3261.



## Inhibition of lipid A-mediated type I interferon induction by Bactericidal/permeability-increasing protein (BPI)

Masahiro Azuma<sup>a</sup>, Aya Matsuo<sup>a</sup>, Yukari Fujimoto<sup>b</sup>, Koichi Fukase<sup>b</sup>, Kaoru Hazeki<sup>c</sup>, Osamu Hazeki<sup>c</sup>, Misako Matsumoto<sup>a</sup>, Tsukasa Seya<sup>a,\*</sup>

<sup>a</sup> Department of Microbiology and Immunology, Hokkaido University Graduate School of Medicine, Kita-15, Nishi-7, Kita-ku Sapporo 060-8638, Japan

<sup>b</sup> Department of Chemistry, Graduate School of Science, Osaka University, Toyonaka, Osaka 560-0043, Japan

<sup>c</sup> Division of Molecular Medical Science, Graduate School of Biomedical Sciences, Hiroshima University, Minami-ku, Hiroshima 734-8551, Japan

Received 31 December 2006

### Abstract

Lipopolysaccharide (LPS), a major constituent of the outer membrane of gram-negative bacteria, consists of polysaccharides and a lipid structure named lipid A. Lipid A is a typical microbial pattern molecule that serves as a ligand for Toll-like receptor 4 (TLR4). TLR4 signals the presence of lipid A to recruit adaptor molecules and induces cytokines and type I interferon (IFN) by activating transcription factor, NF- $\kappa$ B or IRF-3. Here we showed that chemically synthesized TLR4-agonistic lipid A analogs but not antagonistic lipid A activate IFN- $\beta$  in TLR4-expressing HEK293 cells. The amplitude of IFN- $\beta$  promoter activation was in parallel with that of NF- $\kappa$ B. LPS-binding protein (LBP) was required for efficient IFN- $\beta$  induction in this system, and this LBP activity was antagonized by bactericidal/permeability-increasing protein (BPI). Thus, we first show that BPI blocks the TLR4 responses by exogenous administration of BPI to lipid A-sensitive cells. Although the functional mechanism whereby extra-cellular BPI modulates the intra-cellular signal pathways selected by the TLR adaptors, MyD88 and TICAM-1 (TRIF), remains unknown, we infer that the lipid A portion of LPS participates in LBP-amplified IFN- $\beta$  induction and that BPI binding to LPS leads to inhibition of the activation of NF- $\kappa$ B and IFN- $\beta$  by LPS or agonistic lipid A via TLR4 in an extrinsic mode. BPI may serve as a therapeutic potential against endotoxin shock by acting as a regulator for the MyD88- and TICAM-1 pathways in the LPS-TLR4 signaling.

© 2007 Published by Elsevier Inc.

**Keywords:** Toll-like receptor; TICAM-1; Interferon-beta; Chemically synthesized lipid A

Toll-like receptor (TLR) 4 signals the presence of lipopolysaccharide (LPS) which constitutes the outer membrane of gram-negative bacteria and induces proinflammatory cytokines and type I interferons (IFN) [1]. TLR4 also activates the MAP kinase pathway [2] and matures myeloid dendritic cells (mDCs) to conduct professional antigen presentation [3]. Activation of these multiple factors may cause endotoxin shock in patients with sepsis. TLR4 principally triggers two signal pathways initiated by two heterodimeric adaptors, TIRAP (Mal)-MyD88 [1,4]

and TICAM-2 (TRAM)-TICAM-1 (TRIF) [5,6]. The latter TICAM-1 pathway specifically participates in activation of the transcription factor IRF-3 followed by induction of IFN- $\beta$  [5–8].

LPS consists of the core with the antigenic determinant of O antigen and lipid A [9]. Lipid A is a glycolipid consisting of two phosphorylated glucosamines with >4 acylated lipid chains. A number of the structural variations of lipid A have been reported according to the species of bacteria [10]. Majority of the lipid A structures activates host immune response via TLR4, but some of them act as inhibitors for TLR4 signaling [11]. The results were mostly obtained with artificially synthetic lipid A derivatives and NF- $\kappa$ B reporter assay. The ability of these lipid A deriva-

\* Corresponding author. Fax: +81 11 706 7866.  
E-mail address: [seya-tu@pop.med.hokudai.ac.jp](mailto:seya-tu@pop.med.hokudai.ac.jp) (T. Seya).

51 tives to activate the IFN promoter has not been well  
52 characterized.

53 This is partly because LPS-binding protein (LBP) is  
54 required for LPS- or lipid A-mediated type I IFN induction  
55 [12,13]. Blood serum and fetal calf serum (FCS) usually  
56 contain various amounts of LBP, which appears to have  
57 disturbed the determination of accurate potential of LPS/  
58 lipid A to activate the IFN promoter.

59 Bactericidal/permeability-increasing protein (BPI) is a  
60 glycoprotein with pretty high similarity to LBP [14]. BPI  
61 resides in the azurophilic granules of neutrophils and is  
62 secreted into body fluid in response to neutrophil activa-  
63 tion [15]. BPI as well as LBP binds LPS with their N-termi-  
64 nal domains [16]. It has been reported that LBP on one  
65 hand enhances LPS immunomodulatory function, BPI on  
66 the other hand down-regulates LPS function [17]. In the  
67 present study, we tested if BPI inhibits LPS- or lipid A-  
68 mediated type I IFN induction using a variety of synthetic  
69 lipid A compounds.

## 70 Materials and methods

71 *Cells, reagents, and antibodies.* HEK293 and CHO cells were cultured  
72 in DMEM and Ham, respectively, supplemented with heat-inactivated  
73 FCS and antibiotics at 37 °C. In some experiments, human serum depleted  
74 of LBP by the addition of anti-human LBP Ab (R&D Systems, Minne-  
75 apolis, MN) was added to the medium instead of FCS.

76 LPS was purchased from Sigma, St. Louis, MO. Ru.gelatinosus lipid  
77 A, Ru.gelatinosus lipid A-CM-analogue, *Escherichia coli*-type lipid A  
78 and lipid IV<sub>A</sub> were chemically synthesized in Fukase laboratory in  
79 Osaka University, Osaka [18]. PCXN2 vectors for expression of human  
80 LBP and BPI were constructed by H. Nishimura as reported previously  
81 [19]. Antibodies against human LBP and BPI (named D-20) were  
82 purchased from R&D Systems and Santa Cruz biotechnology (Santa  
83 Cruz, CA).

84 *Western blot.* CHO cells were cultured in a 24-well plate for 24 h, and  
85 then transfected with 2 µg of pCXN2/BPI, pCXN2/LBP or empty vectors  
86 (for control). The supernatants were harvested at timed intervals (12, 24,  
87 and 48 h). Proteins in the aliquots were precipitated with methanol and  
88 chloroform [20] and analyzed on SDS-PAGE (10% acrylamide). Briefly,  
89 the aliquots (600 µl) were mixed with 600 µl methanol and 150 µl chlo-  
90 roform and the mixtures were centrifuged at 15,000 rpm for 10 min at  
91 4 °C. The precipitates were suspended in 450 µl of methanol and again  
92 centrifuged at 15,000 rpm for 10 min at 4 °C. The precipitates were dried  
93 in Speedvac and suspended in the SDS-PAGE buffer (60 µl), boiled for  
94 5 min and subjected to SDS-PAGE.

95 After blotting the sample onto nitrocellulose membrane, the mem-  
96 brane was incubated with anti-LBP or anti-BPI mAb (1000-fold diluted)  
97 and then goat anti-mouse IgG Ab (Bio-Rad, 10,000-fold diluted). Proteins  
98 were developed with ECL reagents kit (GE Health Care, Helsinki, Fin-  
99 land) according to the manufacturer's booklet.

100 *Transient transfection and reporter gene assay.* HEK293 cells were  
101 plated on a 6-well plate and transfected with p125-luc reporter or  
102 pELAM-luc (0.5 µg) plasmid, together with the plasmids of TLR4  
103 (0.5 µg), CD14 (0.5 µg), MD2 (0.5 µg) and *Renilla* luciferase reporter  
104 (0.5 ng) using Lipofectamine2000 [21]. Total DNA contents were adjusted  
105 to 2.0 µg by the addition of empty vector. Twenty-four hours later, cells  
106 were harvested, re-plated on a 96-well plate and stimulated with 100 ng/ml  
107 of TLR4 ligands. In some experiments, transfected 293 cells were washed  
108 twice in PBS, suspended in the supernatants of CHO cells (a source of LBP  
109 or BPI) and re-plated on a 96-well plate. Cells were then stimulated with  
110 100 ng/ml of TLR4 ligands. Reporter was measured in 6 h. Experiments  
111 were repeated triplicate at least in three times and a representative one is  
112 shown.

## Results and discussion

113

Lipid A derivatives used in this study were chemically 114  
synthesized as reported previously [22]. Ru.gelatinosus lip- 115  
id A and lipid IV<sub>A</sub> were employed as negative regulators for 116  
NF-κB activation via TLR4 [23], whereas Ru.gelatinosus 117  
lipid A CM-analogue and *E. coli*-type lipid A were as posi- 118  
tive regulators (Fig. 1). LPS was used as a positive control. 119  
The lipid A function was assessed with HEK293 cells 120  
expressing TLR4, MD-2, and CD14 together with the 121  
pELAM promoter (Fig. 2A). The results were principally 122  
consistent with those previously reported using the NF- 123  
κB reporter [24]. LPS, Ru.gelatinosus lipid A CM-ana- 124  
logue and *E. coli*-type lipid A activated the ELAM promot- 125  
er while Ru.gelatinosus lipid A and lipid IV<sub>A</sub> failed to 126  
activate it. IFN-β promoter activation was tested using 127  
the same system transfected with p125-luc instead of the 128  
pELAM (Fig. 2B). LPS and the two positive regulators 129  
of lipid A, but not the two negative regulators of lipid A, 130  
activated p125-luc. The result shown was a representative 131  
of six experiments. Although it is likely from previous 132  
reports that IFN-β-inducing activity is separable from 133  
NF-κB-activation activity in the TLR4 signaling [25], these 134  
two activities are essentially parallel as long as the TLR4 135  
ligand is lipid A derivatives. 136

LBP was reported to discriminate between the two path- 137  
ways for NF-κB and IFN-β [13]. BPI is a paralogue of LBP 138  
and inhibits the LBP function [17]. We next made the sys- 139  
tem for determination of the regulatory activities of LBP 140  
and BPI in terms of the two TLR4 functions on NF-κB 141  
and IFN-β. The LBP and BPI proteins were successfully 142  
secreted out of the CHO cells transfected with their expres- 143  
sion vectors (Fig. 3). Their secretions took a plateau 144  
around 24 h. LBP was ~60 kDa and BPI was ~55 kDa, 145  
consistent with previous reports [12,19]. Their expressions 146  
were similarly efficient: >800 ng/ml within 24 h. Ten milli- 147  
liters of the CHO sup was exchanged for HEK cells with 148  
TLR4/MD-2/CD14 and either of the reporter genes. Then, 149  
the ligand stimulation was added to the HEK293 cells 150  
(Fig. 4A and B). The CHO sup *per se* did not activate 151  
the promoters in the absence of LPS or positive regulators 152  
of lipid A. BPI exerted inhibitory effects on ELAM pro- 153  
moter activation by LPS and to lesser extents by lipid A 154  
(Fig. 4A). ELAM inhibitory rates by the two lipid A deriv- 155  
atives were indistinguishable. In this system, LBP activity 156  
for functional up-regulation of TLR4 was not assigned. 157  
This may reflect the presence of bovine LBP in the CHO 158  
conditioned medium. BPI suppressed LPS-mediated IFN- 159  
β promoter activation (Fig. 4B) as was in NF-κB activa- 160  
tion. BPI, however, less efficiently suppressed IFN-β pro- 161  
moter activation by *E. coli*-type lipid A than by 162  
Ru.gelatinosus lipid A-CM analogue. Addition of LBP 163  
did not result in up-regulation of the IFN-β promoter, also. 164  
However, depletion of serum LBP by mAb-neutralization 165  
(see Materials and methods) resulted in partial loss of 166  
IFN promoter activation by control CHO medium and 167  
the loss of function was recovered by the addition of 168

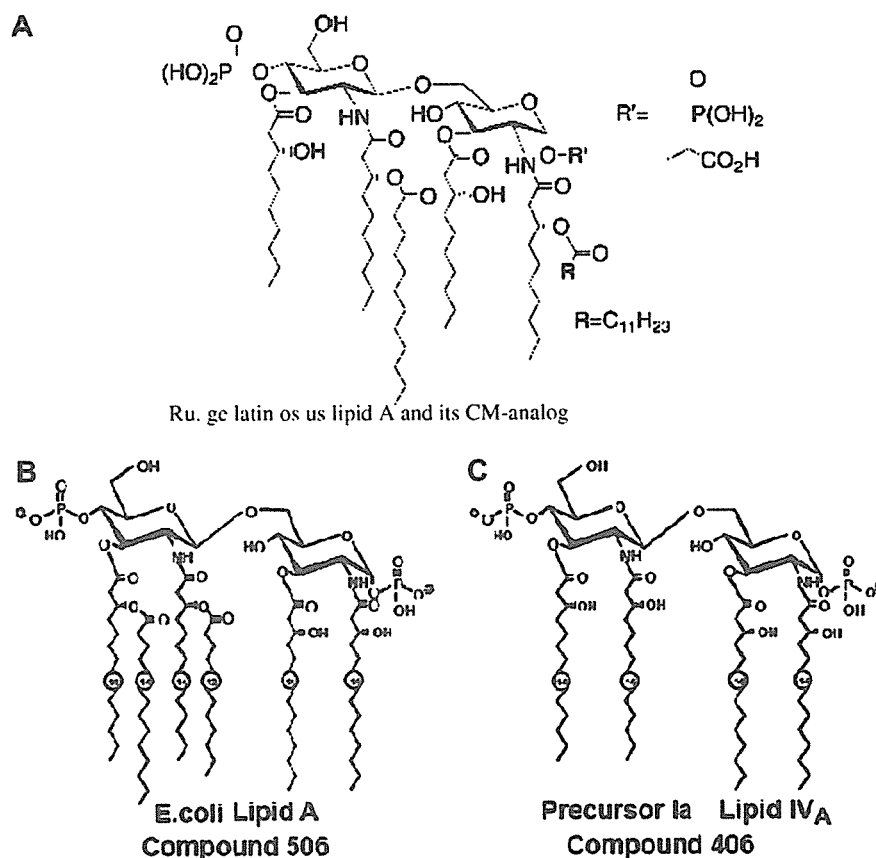


Fig. 1. Structures of lipid A used in this study. Chemically synthesized agonistic and antagonistic lipid A analogs are shown. (A) R' is phosphated in *Ru. gelatinosus* while R' is carboxymethylated in its sCM-analog. (B) *E. coli* lipid A (named compound 506). (C) lipid Iva (named compound 406).

169 CHO medium containing LBP (Fig. 4B, data not shown).  
 170 Thus, BPI serves as an inhibitor against LBP to suppress  
 171 the LPS/lipid A-mediated activation of the IFN- $\beta$  promoter  
 172 as well as NF- $\kappa$ B. The degrees of the BPI inhibitory  
 173 effect appear different among the derivatives of lipid A with  
 174 differential structures.

175 Previous reports suggested the importance of LBP in  
 176 activation of the TICAM-1 pathway leading to IFN- $\beta$   
 177 induction by TLR4 [13]. MD-2, CD14 are essential for sus-  
 178 taining TLR4 function [26]. Our present data can be inter-  
 179 preted to mean that the LPS–LBP complex activates the  
 180 TICAM-1 pathway via presumably binding to the func-  
 181 tional center of TLR4 in the extra-cellular domain, and  
 182 that BPI selectively block the TICAM-1 pathway by com-  
 183 peting LBP for the binding to LPS. If this is the case, the  
 184 extra-cellular molecular events may facilitate the selection  
 185 of the cytoplasmic TLR adaptors leading to activation of  
 186 the IFN pathway. The co-existing LBP plays a major role  
 187 in activation of the TICAM-1 pathway. Our study support-  
 188 ed previous results [13,25,27] and showed that the LPS's  
 189 IFN- $\beta$  inducing activity is endorsed on the lipid A portion.  
 190 Activation of the TICAM-1 pathway is rooted in the func-  
 191 tion of the lipid A moiety as well as the MyD88 pathway,  
 192 and both of the pathways can be blocked by BPI.

Our study furthered the current knowledge on the LBP 193  
 family, LBP and BPI. BPI has just been reported to inhibit 194  
 LBP function by the criteria of NF- $\kappa$ B activation [28]. Here 195  
 we demonstrated that BPI acts as an inhibitor for the 196  
 TICAM-1 pathway of TLR4. Thus, not only the MyD88 197  
 pathway but also the TICAM-1 pathway of TLR4 are 198  
 inhibited by the presence of BPI. BPI is inducible by LPS 199  
 via the TICAM-1 pathway [28] and BPI has >10-fold high- 200  
 er affinity than LBP [29]; secretion of BPI from neutrophils 201  
 even by small amounts may effectively block LBP-mediated 202  
 cytokine/IFN induction by TLR4. BPI would be a regula- 203  
 tor circumventing cytokine storm observed in sepsis. 204

There are many forms of lipid A in bacteria. They elicit 205  
 differential ability for induction of cytokines and IFNs. 206  
 Our results inferred that TLR4-mediated activations of 207  
 NF- $\kappa$ B and IFN- $\beta$  promoter are somewhat differentially 208  
 regulated by BPI according to the differences of the lipid 209  
 A structures. A previous report suggested that endotoxic 210  
 lipid A assembles two sets of TLR4–MD-2 molecules 211  
 resulting in TLR4 dimerization on membrane whereas 212  
 antagonistic lipid A binds a single TLR4–MD-2 complex 213  
 leading to the failure of dimerization. Although the role 214  
 of LBP/BPI in this mechanistic model is unclear, it is likely 215  
 that blocking the formation of dimeric TLR4 also inhibits 216



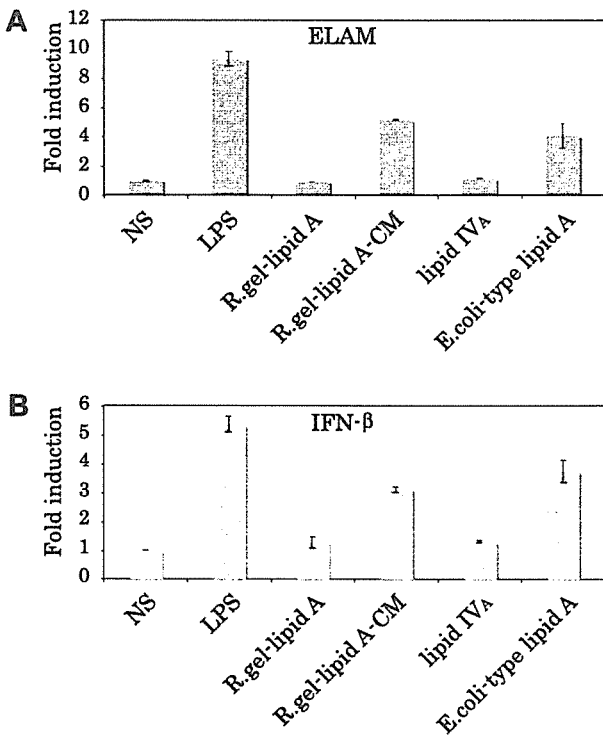


Fig. 2. Activation of NF-κB (A) and the IFN-β promoter (B) by various lipid A derivatives. HEK293 cells were transfected with plasmids for TLR4 assay and either of pELAM-luc or p-125 luc. Twenty-four hours later, cells were added with saline or 100 ng/ml of the indicated TLR4 ligands. phRL-TK was used as a control. Six hours later, cells were collected for reporter assay.

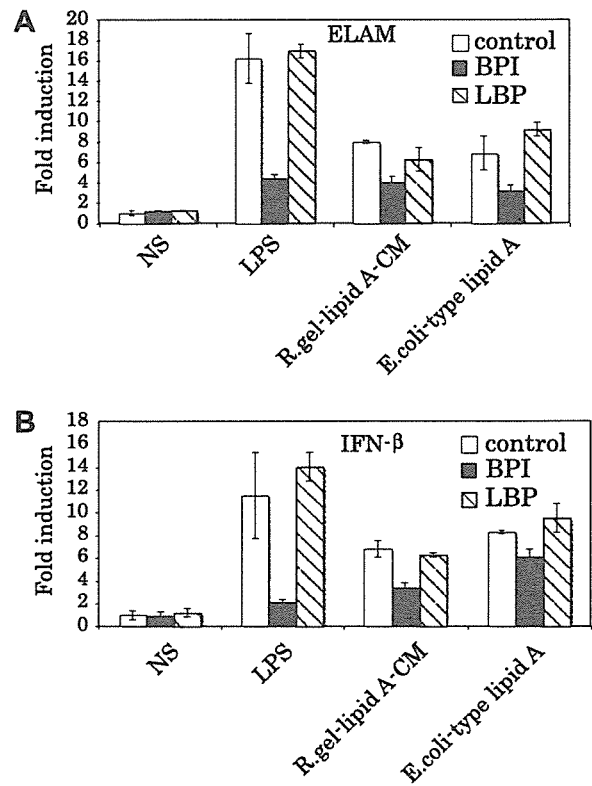


Fig. 4. Inhibition of lipid A-mediated TLR4 activation by BPI. HEK293 cells were transfected with plasmids for TLR4 assay and either of pELAM-luc (A) or p-125 luc (B). Twenty-four hours later, the supernatants of the cells were exchanged with those containing LBP or BPI (see Fig. 3) and the cells were stimulated with TLR4 ligands as in Fig. 2. Six hours later, cells were collected for reporter assay.

217 the TLR4-mediated IFN-inducing pathway. The confor-  
 218 mation of lipid A that confers dimerization on TLR4  
 219 would be crucial for type I IFN induction as well as NF-  
 220 κB [30]. The structure of such acyl moieties in Ru.gelatino-  
 221 sus lipid A may closely link the function of this type of lipid  
 222 A in both NF-κB and IFN-β promoter activation (Fig. 4).  
 223 Although the results are not yet molecularly explained,  
 224 bacteria inducing high average of sepsis may have specific  
 225 lipid A moieties partly resistant to BPI in type I IFN induc-  
 226 tion. These findings suggest that BPI serves as a therapeutic  
 227 potential for septic shock expecting its inhibitory function  
 228 on the TLR4-mediated MyD88- and TICAM-1-pathways.  
 229 Further analysis of the lipid A structures competent to

induction of endotoxin shock will be required in comparison with the susceptibility of the bacterial lipid A to BPI.

**Acknowledgments**

This work was supported in part by CREST, JST (Japan Science and Technology Corporation), by the HCV project in NIH of Japan, and by the Naito Memorial Foundation, Uehara memorial Foundation, Mitsubishi Foundation, Northtic Foundation, and Takeda Foundation. We are

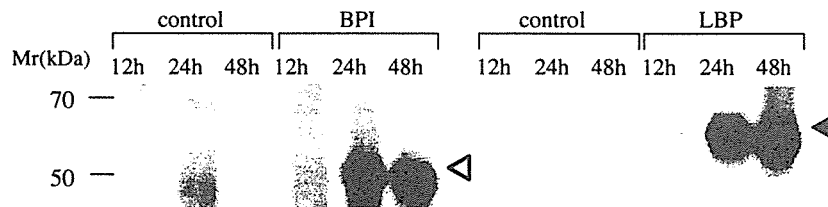


Fig. 3. Secretion of LBP and BPI in CHO cells transfected with their expression vectors. CHO cells were transfected with plasmids for expression of human LBP or BPI. At timed intervals, the supernatants were collected for the test of the secreted proteins. The protein liberated into the supernatants from the transfected cells are shown by Western blotting. See Materials and methods section for detail.

Please cite this article in press as: M. Azuma et al., Inhibition of lipid A-mediated type I interferon induction ..., Biochem. Biophys. Res. Commun. (2007), doi:10.1016/j.bbrc.2007.01.019

238 grateful to Drs. A. Ishii, T. Ebihara, and A. Funami in our  
239 laboratory for their critical discussions.

## 240 References

- 241 [1] S. Akira, M. Yamamoto, K. Takeda, Role of adapters in Toll-like  
242 receptor signalling, *Biochem. Soc. Trans.* 31 (2003) 637–642, Review.  
243 [2] K. Hazeki, H. Masuda, K. Funami, N. Sukenobu, M. Matsumoto, S.  
244 Akira, O. Takeuchi, T. Seya, O. Hazeki, Toll-like receptor-mediated  
245 tyrosine phosphorylation of paxillin via MyD88-dependent and -  
246 independent pathways, *Eur. J. Immunol.* 33 (2003) 740–747.  
247 [3] M. Colonna, B. Pulendran, A. Iwasaki, Dendritic cells at the host-  
248 pathogen interface, *Nat. Immunol.* 7 (2006) 117–120.  
249 [4] N. Sukenobu, K. Hazeki, K. Yoshikawa, T. Yamamoto, U. Kikk-  
250 awa, M. Matsumoto, T. Seya, O. Hazeki, Protein kinase Cd  
251 associates TIRAP/Mal and regulates NF- $\kappa$ B and mitogen-activated  
252 protein kinases in Toll-like receptor signaling, *Mol. Immunol.*, in  
253 press.  
254 [5] H. Oshiumi, M. Matsumoto, K. Funami, T. Akazawa, T. Seya,  
255 TICAM-1, an adapter molecule that participates in Toll-like receptor  
256 3-mediated interferon-beta induction, *Nat. Immunol.* 4 (2003) 161–  
257 167.  
258 [6] H. Oshiumi, K. Shida, M. Sasai, T. Fujita, M. Matsumoto, T. Seya,  
259 TIR-containing adapter molecule(TICAM)-2, a bridging adapter  
260 recruiting to Toll-like receptor 4 TICAM-1 that induces interferon-  
261 beta, *J. Biol. Chem.* 278 (2003) 49751–49762.  
262 [7] K.A. Fitzgerald, D.C. Rowe, B.J. Barnes, D.R. Caffrey, A. Visintin,  
263 E. Latz, B. Monks, P.M. Pitha, D.T. Golenbock, LPS-TLR4  
264 signaling to IRF-3/7 and NF-kappaB involves the toll adapters  
265 TRAM and TRIF, *J. Exp. Med.* 198 (2003) 1043–1055.  
266 [8] M. Yamamoto, S. Sato, H. Hemmi, K. Hoshino, T. Kaisho, H.  
267 Sanjo, O. Takeuchi, M. Sugiyama, M. Okabe, K. Takeda, S. Akira,  
268 Role of adaptor TRIF in the MyD88-independent toll-like receptor  
269 signaling pathway, *Science* 301 (2003) 640–643.  
270 [9] C.R.H. Raetz, *Biochemistry of endotoxins*, *Annu. Rev. Biochem.* 59  
271 (1990) 129–170.  
272 [10] A. Christian, Z. Ulrich, Chemical structure of Lipid A—The primary  
273 immunomodulatory center of bacterial lipopolysaccharides, *Trends*  
274 *Glycosci. Glycotechnol.* 14 (2002) 69–86.  
275 [11] W.J. Christ, O. Asano, A.L. Robidoux, M. Perez, Y. Wang, G.R.  
276 Dubuc, W.E. Gavin, L.D. Hawkins, P.D. McGuinness, M.A.  
277 Mullarkey, E5531, a pure endotoxin antagonist of high potency,  
278 *Science* 268 (1995) 80–83.  
279 [12] R.R. Schumann, S.R. Leong, G.W. Flaggs, P.W. Gray, S.D. Wright,  
280 J.C. Mathison, P.S. Tobias, R.J. Ulvitch, Structure and function of  
281 lipopolysaccharide binding protein, *Science* 249 (1990) 1429–1431.  
282 [13] A. Kato, T. Ogasawara, T. Homma, H. Saito, K. Matsumoto,  
283 Lipopolysaccharide-binding protein critically regulates lipopolysac-  
284 charide-induced IFN-beta signaling pathway in human monocytes, *J.*  
285 *Immunol.* 172 (2004) 6185–6194.  
286 [14] J. Weiss, K. Muello, M. Victor, P. Elsbach, The role of lipopolysac-  
287 charides in the action of the bactericidal/permeability-increasing  
288 neutrophil protein on the bacterial envelope, *J. Immunol.* 132 (1984)  
289 3109–3115.  
290 [15] M.N. Marra, C.G. Wilde, M.S. Collins, J.L. Snable, M.B. Thornton,  
291 R.W. Scott, The role of bactericidal/permeability-increasing protein  
292 as a natural inhibitor of bacterial endotoxin, *J. Immunol.* 148 (1992)  
293 532–537.  
294 [16] C.E. Ooi, J. Weiss, P. Elsbach, B. Frangione, B. Mannion, A 25-kDa  
295 NH2-terminal fragment carries all the antibacterial activities of the  
human neutrophil 60-kDa bactericidal/permeability-increasing pro-  
tein, *J. Biol. Chem.* 262 (1987) 14891–14894.  
[17] J. Weiss, Bactericidal/permeability-increasing protein (BPI) and  
lipopolysaccharide-binding protein (LBP): structure, function and  
regulation in host defence against Gram-negative bacteria, *Biochem*  
*Soc. Trans.* 31 (2003) 785–790.  
[18] K. Fukase, Y. Fukase, M. Oikawa, W.C. Liu, Y. Suda, S. Kusumoto,  
Divergent synthesis and biological activities of lipid A analogs of  
shorter acyl chains, *Tetrahedron Lett.* 54 (1998) 4033–5050.  
[19] H. Nishimura, A. Gogami, Y. Miyagawa, A. Nanbo, Y. Murakami,  
T. Baba, S. Nagasawa, Bactericidal/permeability-increasing protein  
promotes complement activation for neutrophil-mediated phagocy-  
tosis on bacterial surface, *Immunology* 103 (2001) 519–525.  
[20] D. Wessel, U.I. Flugge, A method for the quantitative recovery of  
protein in dilute solution in the presence of detergents and lipids,  
*Anal. Biochem.* 138 (1984) 141–143.  
[21] M. Sasai, H. Oshiumi, M. Matsumoto, N. Inoue, F. Fujita, M.  
Nakanishi, T. Seya, Cutting Edge: NF- $\kappa$ B-activating kinase-associ-  
ated protein 1 participates in TLR3/Toll-IL-1 homology domain-  
containing adapter molecule-1-mediated IFN Regulatory Factor 3  
activation, *J. Immunol.* 174 (2005) 27–30.  
[22] Y. Fujimoto, Y. Adachi, M. Akamatsu, Y. Fukase, M. Kataoka, Y.  
Suda, K. Fukase, S. Kusumoto, Synthesis of lipid A and its analogues  
for investigation of the structural basis for their bioactivity, *J.*  
*Endotoxin Res.* 11 (2005) 341–347.  
[23] S. Saitoh, S. Akashi, T. Yamada, N. Tanimura, M. Kobayashi, K.  
Konno, F. Matsumoto, K. Fukase, S. Kusumoto, Y. Nagai, Y.  
Kusumoto, A. Kosugi, K. Miyake, Lipid A antagonist, lipid IVa, is  
distinct from lipid A in interaction with Toll-like receptor 4 (TLR4)-  
MD-2 and ligand-induced TLR4 oligomerization, *Int. Immunol.* 16  
(2004) 961–969.  
[24] J.C. Chow, D.W. Young, D.T. Golenbock, W.J. Christ, F. Gusovsky,  
Toll-like receptor-4 mediates lipopolysaccharide-induced signal tran-  
sduction, *J. Biol. Chem.* 274 (1999) 10689–10692.  
[25] S. Doyle, S. Vaidya, R. O'Connell, H. Dadgostar, P. Dempsey, T.  
Wu, G. Rao, R. Sun, M. Haberland, R. Modlin, G. Cheng, IRF3  
mediates a TLR3/TLR4-specific antiviral gene program, *Immunity* 17  
(2002) 251–263.  
[26] S. Akashi, S. Saitoh, Y. Wakabayashi, T. Kikuchi, N. Takamura, Y.  
Nagai, Y. Kusumoto, K. Fukase, S. Kusumoto, Y. Adachi, A.  
Kosugi, K. Miyake, Lipopolysaccharide interaction with cell surface  
Toll-like receptor 4-MD-2: higher affinity than that with MD-2 or  
CD14, *J. Exp. Med.* 198 (2003) 1035–1042.  
[27] M. Sasai, M. Shingai, K. Funami, M. Yoneyama, T. Fujita, M.  
Matsumoto, T. Seya, NAPI (NAK-associated protein 1) participates  
in both the TLR3 and the cytoplasmic pathways in type I interferon  
induction, *J. Immunol.* 177 (2006) 8676–8683.  
[28] M. Eckert, I. Wittmann, M. Rollinghoff, A. Gessner, M. Schnare,  
Endotoxin-induced expression of murine bactericidal permeability/  
increasing protein is mediated exclusively by toll/IL-1 receptor  
domain-containing adaptor inducing IFN-beta-dependent pathways,  
*J. Immunol.* 176 (2006) 522–528.  
[29] C.G. Wilde, J.J. Seilhamer, M. McGrogan, N. Ashton, J.L. Snable,  
J.C. Lane, S.R. Leong, M.B. Thornton, K.L. Miller, R.W. Scott,  
M.N. Marra, Bactericidal/permeability-increasing protein and lipo-  
polysaccharide (LPS)-binding protein. LPS binding properties and  
effects on LPS-mediated cell activation, *J. Biol. Chem.* 262 (1994)  
17411–17416.  
[30] U. Seydel, M. Oikawa, K. Fukase, S. Kusumoto, K. Brandenburg,  
Intrinsic conformation of lipid A is responsible for agonistic and  
antagonistic activity, *Eur. J. Biochem.* 267 (2000) 3032–3039.

# TLR3-Mediated Synthesis and Release of *Eotaxin-1/CCL11* from Human Bronchial Smooth Muscle Cells Stimulated with Double-Stranded RNA<sup>1</sup>

Kyoko Niimi,<sup>\*†</sup> Koichiro Asano,<sup>2\*†</sup> Yoshiki Shiraishi,<sup>\*†</sup> Takeshi Nakajima,<sup>\*†</sup> Misa Wakaki,<sup>\*†</sup> Junko Kago,<sup>\*†</sup> Takahisa Takihara,<sup>\*†</sup> Yusuke Suzuki,<sup>\*</sup> Koichi Fukunaga,<sup>\*</sup> Tetsuya Shiomi,<sup>\*</sup> Tsuyoshi Oguma,<sup>\*</sup> Koichi Sayama,<sup>\*</sup> Kazuhiro Yamaguchi,<sup>\*</sup> Yukikazu Natori,<sup>‡</sup> Misako Matsumoto,<sup>§</sup> Tsukasa Seya,<sup>§</sup> Mutsuo Yamaya,<sup>¶</sup> and Akitoshi Ishizaka<sup>\*†</sup>

Respiratory infections with RNA viruses, such as rhinovirus or respiratory syncytial virus, are a major cause of asthma exacerbation, accompanied by enhanced neutrophilic and/or eosinophilic inflammation of the airways. We studied the effects of dsRNA synthesized during RNA virus replication, and of its receptor, TLR3, on the synthesis of eosinophilic chemokines in bronchial smooth muscle cells (BSMC). Synthetic dsRNA, polyinosinic-cystidic acid (poly(I:C)), induced the synthesis of eosinophilic chemokines, eotaxin-1/CCL11 and RANTES/CCL5, from primary cultures of human BSMC, and IL-4 increased synergistically the synthesis of poly(I:C)-induced CCL11. A robust eosinophil chemotactic activity was released from BSMC stimulated with poly(I:C) and IL-4, which was mostly inhibited by preincubation with an anti-CCL11, but not with an anti-CCL5 Ab. Although the immunoreactivity of TLR3 was detectable on the cellular surface of BSMC by flow cytometric analysis, pretreatment with an anti-TLR3-neutralizing Ab failed to block the poly(I:C)-induced synthesis of CCL11. We have determined by confocal laser-scanning microscopy that the immunoreactivity of TLR3 was aggregated intracellularly in poly(I:C)-stimulated BSMC, colocalizing with fluorescein-labeled poly(I:C). The synthesis of *CCL11* was prominently inhibited by the transfection of TLR3-specific small interfering RNA or by bafilomycin A1, an endosomal acidification inhibitor, further supporting the essential role played by intracellular TLR3 in the synthesis of poly(I:C)-induced *CCL11* in BSMC. In conclusion, these observations suggest that, by activating intracellular TLR3 in BSMC, respiratory RNA virus infections stimulate the production of *CCL11* and enhance eosinophilic inflammation of the airways in the Th2-dominant microenvironment. *The Journal of Immunology*, 2007, 178: 489–495.

Acute exacerbations of asthma, characterized by disease manifestations such as wheezing and dyspnea, seriously disturb the quality of life of susceptible patients. The episodes are accompanied by worsening of airflow limitations; bronchial hyperresponsiveness; and increased neutrophilic, lymphocytic, and/or eosinophilic inflammation of the airways. Respiratory RNA viral infections are a major cause of acute exacerbation of asthma, and positive-sense ssRNA viruses, such as rhinovirus and coronavirus, are often isolated in the airways of adults during exacerbations, whereas negative-sense ssRNA viruses, including respiratory syncytial virus (RSV)<sup>3</sup> and para-

influenza virus, are the main pathogens causing wheezing bronchiolitis in children (1, 2).

Eosinophils play an important role in the virus-induced deterioration of asthma. The number of eosinophils and the concentration of eosinophil cationic protein in induced sputum have been correlated with an increase in bronchial responsiveness during experimental rhinovirus infections in adult asthmatics (3). A marked eosinophilic inflammation of the airways was observed in a substantial proportion of children with RSV bronchiolitis (4, 5), and the pathologic changes in the airways of mice with RSV infection mimicked eosinophilic bronchiolitis in humans, especially in allergen-sensitized and exposed animals (6, 7).

The induction of eosinophilic chemokine synthesis is one of the putative triggering mechanisms of eosinophilia in the airways during viral infection. Infections of respiratory epithelial cells with rhinovirus, RSV, or influenza virus are associated with the production of chemokines, such as eotaxin-1/CCL11 and RANTES/CCL5 (8–11). Eosinophilic inflammation in RSV-infected mice was accompanied by the production of CCL11 and MCP-3/CCL7, and was markedly reduced by treatment with an anti-CCL11 Ab (12, 13).

It has been demonstrated that dsRNA, as a virus genome fragment or as a replicative intermediate of RNA virus (14), induces the production of chemokines, such as CCL5, MCP-1/CCL2, eotaxin-3/CCL26, IL-8/CXCL8, and IFN-inducible protein-10/CXCL10 in respiratory epithelial cells (15–20). TLR3, a receptor for dsRNA, is expressed in respiratory epithelial cells, as well as in dendritic cells, mast cells, and fibroblasts (21–23). Bronchial smooth muscle cells (BSMC) are another major source of chemokines, including CCL5 and CCL11 (24–26), although little is known regarding the expression of TLR3 and responsiveness to

\*Division of Pulmonary Medicine, Department of Medicine, Keio University School of Medicine, Tokyo, Japan; <sup>†</sup>Keio-Pfizer Research Laboratories, Shinanomachi Campus Research Park, Keio University School of Medicine, Tokyo, Japan; <sup>‡</sup>RNAi, Tokyo, Japan; <sup>§</sup>Department of Microbiology and Immunology, Graduate School of Medicine, Hokkaido University, Sapporo, Japan; and <sup>¶</sup>Department of Geriatrics and Gerontology, Tohoku University School of Medicine, Sendai, Japan

Received for publication January 24, 2006. Accepted for publication October 16, 2006.

The costs of publication of this article were defrayed in part by the payment of page charges. This article must therefore be hereby marked *advertisement* in accordance with 18 U.S.C. Section 1734 solely to indicate this fact.

<sup>1</sup> This study was supported in part by a Grant-in-Aid from the Ministry of Education, Culture, Sports, Science, and Technology.

<sup>2</sup> Address correspondence and reprint requests to Dr. Koichiro Asano, Division of Pulmonary Medicine, Department of Medicine, Keio University School of Medicine, 35 Shinanomachi, Shinjuku-ku, Tokyo 160-8582, Japan. E-mail address: ko-asano@qa2.so-net.ne.jp

<sup>3</sup> Abbreviations used in this paper: RSV, respiratory syncytial virus; BSMC, bronchial smooth muscle cell; EEA-1, early endosome Ag 1; poly(I:C), polyinosinic-cystidic acid; siRNA, small interfering RNA.

Copyright © 2006 by The American Association of Immunologists, Inc. 0022-1767/06/\$2.00

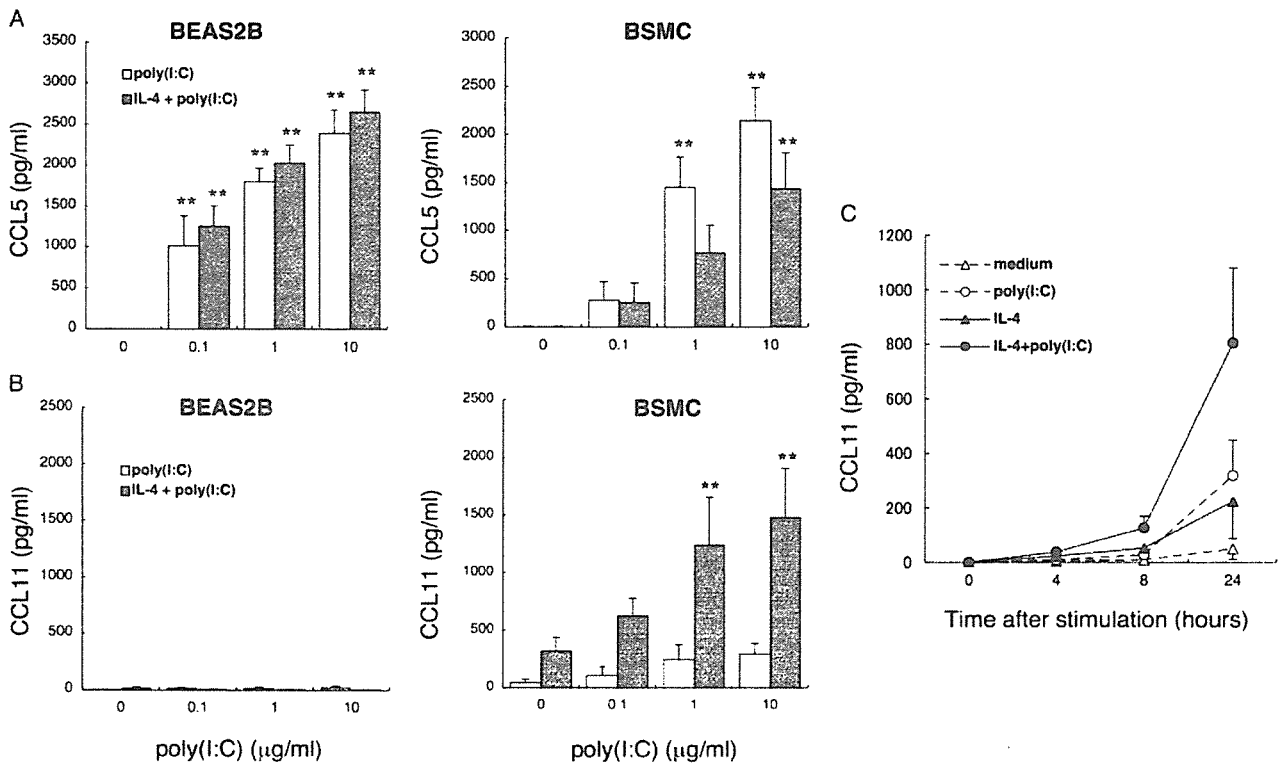


**FIGURE 1.** RANTES/CCL5 (A) and eotaxin-1/CCL11 (B) concentrations in the culture supernatant of poly(I:C)-stimulated BEAS2B cells and BSMC. Cells were stimulated with poly(I:C) (0.1–10  $\mu\text{g/ml}$ ) for 24 h in presence or absence of 10 ng/ml IL-4. Mean  $\pm$  SEM from three duplicate experiments (BEAS2B), or four duplicate experiments using BSMC from different donors. \*\*,  $p < 0.005$  compared with the cells not stimulated with poly(I:C). C, Kinetics of CCL11 release from BSMC stimulated with 10  $\mu\text{g/ml}$  poly(I:C), or 10 ng/ml IL-4, or both. Mean  $\pm$  SEM from four duplicate experiments using BSMC from different donors.

dsRNA in this cell type. Therefore, we have examined, using primary cultures of human BSMC, the following: 1) whether dsRNA induces the production of eosinophilic chemokines and eosinophil chemotactic activity; 2) whether TLR3 is expressed in BSMC and its subcellular localization; and 3) whether the dsRNA-induced chemokine synthesis in BSMC is mediated by TLR3.

## Materials and Methods

### Cell culture

Primary cultures of normal human BSMC were obtained from Cambrex, and cultured in medium containing 5% FBS; 1 ng/ml human recombinant epidermal growth factor; 2 ng/ml fibroblast growth factor; and 10  $\mu\text{g/ml}$  insulin, gentamicin, and amphotericin B. BSMC from three to five different donors, at the fourth to sixth passage, were used for the experiments. A BEAS2B airway epithelial cell line was obtained from American Type Culture Collection, and maintained in DMEM/F12K medium containing 10% FBS.

### Measurements of CC chemokine release

Confluent BSMC or BEAS2B cells in 24-well plates were starved in absence of FBS and growth factors for 24 h, then stimulated with polyinosinic-cytidylic acid (poly(I:C); Amersham Biosciences) for a designated period of time, in presence or absence of 10 ng/ml IL-4 (PeproTech) or 10 ng/ml IL-13 (R&D Systems). The concentration of CCL5, CCL11, CXCL8, CXCL10, and IL-6 in the culture supernatant was measured by ELISA (R&D Systems), according to the manufacturer's instructions.

### Quantitative RT-PCR

Total RNA was extracted from BSMC with an RNeasy Mini Kit (Qiagen). The amounts of *CCL11* and *TLR3* transcripts were determined by reverse transcription using SuperScript II (Invitrogen Life Technologies), followed by quantitative PCR amplification by the TaqMan method (ABI PRISM 7000; Applied Biosystems). The comparative threshold cycle method was

validated and used to interpret the results. Premixed PCR primers and TaqMan probes for human *CCL11*, *TLR3*, and *GAPDH* (Assay-on-Demand) were obtained from Applied Biosystems. Conditions for PCR were as follows: 1 cycle at 95°C for 9 min, 50 cycles at 95°C for 0.5 min, 60°C for 1 min, and 1 cycle at 72°C for 5 min.

### Purification of peripheral blood eosinophils

Peripheral blood eosinophils were isolated from nonatopic healthy subjects, as described previously (27). Briefly, RBC were removed from 40 ml of heparinized peripheral blood using Dextran T-500 (Pharmacia) and mononuclear cells by centrifugation over 1.083 g/ml Histopaque (Sigma-Aldrich). After hypotonic cell lysis to remove any remaining RBC, neutrophils were removed by a CD16-negative selection method, using CD16-labeled magnetic microbeads (Miltenyi Biotec) and autoMACS (Miltenyi Biotec). Eosinophils (99  $\pm$  1%, mean  $\pm$  SEM) were resuspended in RPMI 1640 supplemented with 10% FBS.

### Chemotactic activity for eosinophils

Confluent BSMC in six-well plates, growth arrested without FBS and growth factors for 24 h, were stimulated with 10  $\mu\text{g/ml}$  poly(I:C), or 10 ng/ml IL-4, or both. Culture supernatants were collected 24 h later, centrifuged for 15 min at 3000 rpm at 4°C, and stored at  $-80^\circ\text{C}$  for the subsequent experiments. In the chemokine-neutralizing experiments, the culture supernatant was incubated with 10  $\mu\text{g/ml}$  anti-CCL11-neutralizing Ab (R&D Systems), 10  $\mu\text{g/ml}$  anti-CCL5 Ab (R&D Systems), or both, at 37°C, for 1 h before the assay.

Eosinophil chemotactic activity was examined using a slightly modified method described previously (27, 28). In brief, 300  $\mu\text{l}$  of culture supernatants diluted 8-fold, or standard eosinophils ( $5 \times 10^2$ – $3 \times 10^4$  cells/well) were added to the lower compartment of a 96-well chemotaxis plate separated by a 3- $\mu\text{m}$ -pore-size filter (NeuroProbe), and eosinophils (50  $\mu\text{l}$ ,  $10^6$  cells/ml) were placed in the upper compartment. After 1 h of incubation at 37°C, the medium on the upper surface of the filter was wiped and replaced by 0.5 mM EDTA in PBS. After another hour of incubation, the plate was centrifuged at 1500 rpm at 4°C for 20 min, the filter was gently removed, and the supernatant was aspirated. The eosinophil peroxidase activity in the